[6] J.H. Hu, H. Zhang, R. Wagey, C. Krieger, S.L. Pelech, Protein kinase and protein phosphatase expression in amyotrophic lateral sclerosis spinal cord, J. Neurochem. 85 (2003) 432–442.
[7] N.V. Jammi, L.R. Whitby, P.A. Beal, Small molecule inhibitors of the RNA-dependent protein kinase, Biochem. Biophys. Res. Commun. 308 (2003) 50–57.
[8] R.J. Kaufman, Stress signaling from the lumen of the endoplasmic reticulum: coordination of gene transcriptional and translational controls, Genes Dev. 13 (1999) 1211–1233.
[9] W. Maruyama, Y. Akao, M.C. Carrillo, K. Kitani, M.B. Youdium, M. Naoi, Neuroprotection by propargylamines in Parkinson's disease: suppression of apoptosis and induction of prosurvival genes, Neurotoxicol. Teratol. 24 (2002) 675–682.
[10] H. Nishitoh, A. Matsuzawa, K. Tobiume, K. Saegusa, K. Takeda, K. Inoue, S. Hori, A. Kakizuka, H. Ichijo, ASK1 is essential for endoplasmic reticulum stress-induced neuronal cell death triggered by expanded polyglutamine repeats, Genes Dev. 16 (2002) 1345–1355.
[11] H. Nishitoh, M. Saitoh, Y. Mochida, K. Takeda, H. Nakano, M. Rothe, K. Miyazono, H. Ichijo, ASK1 is essential for JNK/SAPK activation by TRAF2, Mol. Cell 2 (1998) 389–395.
[12] R. Onuki, Y. Bando, E. Suyama, T. Katayama, H. Kawasaki, T. Baba, M. Tohyama, K. Taira, An RNA-dependent protein kinase is involved in tunicamycin-induced apoptosis and Alzheimer's disease, EMBO. J. 23 (2004) 959–968.
[13] A.L. Peel, R.V. Rao, B.A. Cottrell, M.R. Hayden, L.M. Ellerby, D.E. Bredesen, Double-stranded RNA-dependent protein kinase, PKR, binds preferentially to Huntington's disease (HD) transcripts and is activated in HD tissue, Hum. Mol. Genet. 10 (2001) 1531–1538.
[14] S.P. Srivastava, K.U. Kumar, R.J. Kaufman, Phosphorylation of eukaryotic translation initiation factor 2 mediates apoptosis in response to activation of the double-stranded RNA-dependent protein kinase, J. Biol. Chem. 273 (1998) 2416–2423.
[15] K.C. Suen, M.S. Yu, K.F. So, R.C. Chang, J. Hugon, Upstream signaling pathways leading to the activation of double-stranded RNA-dependent serine/threonine protein kinase in beta-amyloid peptide neurotoxicity, J. Biol. Chem. 278 (2003) 49819–49827.
[16] T. Takizawa, C. Tatematsu, Y. Nakanishi, Double-stranded RNA-activated protein kinase interacts with apoptosis signal-regulating kinase 1. Implications for apoptosis signaling pathways, Eur. J. Biochem./FEBS 269 (2002) 6126–6132.
[17] S. Wu, R.J. Kaufman, A model for the double-stranded RNA (dsRNA)-dependent dimerization and activation of the dsRNA-activated protein kinase PKR, J. Biol. Chem. 272 (1997) 1291–1296.

Molecular Vision 2007; 13:578-87 <http://www.molvis.org/molvis/v13/a62/>
Received 26 October 2006 | Accepted 28 March 2007 | Published 5 April 2007

Involvement of ER stress in retinal cell death

Masamitsu Shimazawa,[1] Yuta Inokuchi,[1] Yasushi Ito,[1] Hiroshi Murata,[2] Makoto Aihara,[2] Masayuki Miura,[3] Makoto Araie,[2] Hideaki Hara[1]

[1]Department of Biofunctional Molecules, Gifu Pharmaceutical University, Gifu, [2]Department of Ophthalmology, University of Tokyo School of Medicine, Tokyo, [3]Department of Genetics, Graduate School of Pharmaceutical Sciences, University of Tokyo, Tokyo, Japan

Purpose: To clarify whether endoplasmic reticulum (ER) stress is involved in retinal cell death, using cultured retinal ganglion cells (RGC-5, a rat ganglion cell line transformed with E1A virus), and transgenic mice ER stress-activated indicator (ERAI) mice carrying a human XBP1 and venus a variant of green fluorescent protein (GFP) fusion gene.

Methods: RGC-5 damage was induced by tunicamycin, and cell viability was measured by double nuclear staining (Hoechst 33342 and either YO-PRO-1 or propidium iodide). The expressions of glucose-regulated protein 78(GRP78)/BiP, the phosphorylated form of eukaryotic initiation factor 2α (p-eIF2α), and C/EBP-homologous (CHOP) protein after tunicamycin (in vitro or in vivo) or *N*-methyl-D-aspartate (NMDA; in vivo) treatment were measured using immunoblot or immunostaining. ERAI mice carrying the F-XBP1-DBD-venus expression gene were used to monitor ER-stress in vivo. Twenty-four hours after intravitreal injection of tunicamycin or NMDA, or after raising intraocular pressure (IOP), the retinal fluorescence intensity was visualized in anesthetized animals using an ophthalmoscope and in retinal flatmount or cross-section specimens using laser confocal microscopy.

Results: Treatment with tunicamycin induced apoptotic cell death in RGC-5 and also induced production of ER stress-related proteins (BiP, the phosphorylated form of eIF2α, and CHOP protein). In vivo, tunicamycin induced retinal ganglion cell (RGC) loss and thinning of the inner plexiform layer, 7 days after intravitreal injection. In flatmounted retinas of ERAI mice, the fluorescence intensity arising from the XBP-1-venus fusion protein, indicating ER-stress activation, was increased at 24 h after tunicamycin, NMDA, or IOP elevation. In transverse cross-sections from ERAI mice, the fluorescence intensity was first increased in cells of the ganglion cell and inner plexiform layers at 12 and 24 h, respectively, after NMDA injection, and it was localized to ganglion and amacrine cells at 12 and 24 h, respectively, and to microglial cells at 72 h. BiP and CHOP were increased at 12 h after NMDA injection, and the increases persisted for the remainder of the 72 h observation period.

Conclusions: These data indicate that ER-stress may play a pivotal role in RGC death, whether induced by NMDA or IOP elevation.

Endoplasmic reticulum (ER) stress is caused by a number of biochemical and physiological stimuli that result in the accumulation of unfolded proteins in the ER lumen, and it is closely associated with the neuronal cell injury caused by vascular and neurodegenerative diseases such as stroke, Alzheimer disease, and Parkinson disease [1-3]. However, little is known about the role, if any, of ER stress in retinal damage.

Retinal ganglion cell (RGC) death is a common feature of many ophthalmic disorders such as glaucoma, optic neuropathies, and retinovascular diseases, such as diabetic retinopathy and retinal vein occlusions. RGC death has been reported to occur via a variety of mechanisms involving, for example, oxidative stress [4], excitatory amino acids [5], nitric oxide (NO) [6], and apoptosis [7]. Glutamate, one of the excitatory amino acids, is the main neurotransmitter in the retinal signaling pathway. Excessive glutamate increases both intracellular Ca^{2+} and NO production through activation of the *N*-methyl-D-aspartate (NMDA)-type glutamate receptor, resulting in retinal cell death [8,9]. Recently, Uehara et al. [10] reported that in primary cortical culture, even mild exposure of NMDA induces apoptotic cell death. They demonstrated to be caused by an accumulation of polyubiquitinated proteins and increases in X box binding protein (XBP-1) mRNA splicing and C/EBP-homologous (CHOP) mRNA, representing activation of the unfolded-protein response (UPR) signaling pathway. They also found that protein-disulphide isomerase (PDI), which assists in the maturation and transport of unfolded secretory proteins, prevented the neurotoxicity associated with ER stress. They suggest that neurodegenerative disorders might be mediated by *S*-nitrosylation of PDI, which would reduce its enzymatic activity. Their results strongly suggest that activation of ER stress may participate in the retinal cell death occurring after NMDA receptor activation and/or ischemic insult. Hence, the purpose of the present study is to examine how ER stress might induce retinal damage both in vitro using cultured retinal ganglion cells (RGC-5, a rat ganglion cell line transformed using E1A virus) and in vivo (using ER stress-activated indicator (ERAI) transgenic mice, in which effective identification of cells under ER-stress conditions is possible in vivo, as described in our previous report) [11]. Use of ERAI mice should provide valuable information regarding the dynamics of ER stress-induced retinal damage.

Correspondence to: Dr. Hideaki Hara, Ph.D., Department of Biofunctional Molecules, Gifu Pharmaceutical University, 5-6-1 Mitahora-higashi, Gifu 502-8585, Japan; Phone: +81-58-237-8596; FAX: +81-58-237-8596, email: hidehara@gifu-pu.ac.jp

METHODS

Materials: Dulbeco's modified Eagles's medium (D-MEM) was purchased from Sigma-Aldrich (St. Louis, MO). The drugs used and their sources were as follows. Tunicamycin was obtained from Calbiochem (San Diego, CA) and Wako (Osaka, Japan). Isoflurane was acquired from Nissan Kagaku (Tokyo, Japan), and fetal bovine serum (FBS) was obtained from Valeant (Costa Mesa, CA).

Retinal ganglion cell line (retinal ganglion cell-5) culture: Cultures of RGC-5 were maintained in D-MEM supplemented with 10% FBS, 100 U/ml penicillin (Meiji Seika Kaisha, Ltd., Tokyo, Japan), and 100 µg/ml streptomycin (Meiji Seika Kaisha, Ltd.) in a humidified atmosphere of 95% air and 5% CO_2 at 37 °C. The RGC-5 cells were passaged by trypsinization every 3 days, as in a previous report [12].

Cell viability assay after tunicamycin: RGC-5 cells were plated at a density of 1000 cells/well in 96-well culture plates (number 3072, Falcon®, Becton Dickinson and Company, Franklin Lakes, NJ). Twenty-four h later, cells were washed twice with D-MEM and then immersed in D-MEM supplemented with 1% FBS plus tunicamycin at 1 to 4 µg/ml. Twenty-four or forty-eight hours after the addition of tunicamycin, cell viability was measured using a single-cell digital imaging-based method employing fluorescent staining of nuclei. Briefly, cell death was assessed on the basis of combination staining with fluorescent dyes [namely, Hoechst 33342 (Molecular Probes, Eugene, OR) and either YO-PRO-1 (Molecular probes) or propidium iodide (PI; Molecular probes)]. Observations were made using an Olympus IX70 inverted epifluorescence microscope (Olympus, Tokyo, Japan). At the end of the above culture period, Hoechst 33342 and YO-PRO-1 or PI dyes were added to the culture medium at 8 µM, 0.1 µM, and 1.5 µM, respectively, for 30 min. Images were collected using a digital camera (Coolpix 4500, Nikon Corp., Tokyo, Japan). In a blind manner, a total of at least 400 cells per condition were counted using image-processing software (Image-J ver. 1.33f, National Institutes of Health, Bethesda, MD). Cell mortality was quantified by expressing the number of YO-PRO-1- or PI-positive cells as a percentage of the number of Hoechst 33342-positive cells.

Animals: ER-stress-activated indicator (ERAI)-transgenic mice carrying the F-XBP1DDBD-venus expression gene [11] and their background wild-type mice (C57BL/6) aged 8-11 weeks or male adult ddY mice (Japan SLC, Hamamatsu, Japan) weighing 36-43 g for experiments other than the comparison with ERAI-transgenic mice were used, and were kept under controlled lighting conditions (12 h:12 h light/dark). All experiments were performed in accordance with the ARVO statement for the Use of Animals in Ophthalmic and Vision Research, and were approved and monitored by the Institutional Animal Care and Use Committee of Gifu Pharmaceutical University.

Retinal damage induced by N-methyl-D-aspartate (NMDA)-, tunicamycin-, or intraocular pressure (IOP) elevation: Male mice were anesthetized with 3.0% isoflurane and maintained using 1.5% isoflurane in 70% N_2O and 30% O_2, delivered via an animal general anesthesia machine (Soft Lander, Sin-ei industry Co. Ltd., Saitama, Japan). The body temperature was maintained at 37.0 - 37.5 °C with the aid of a heating pad and heating lamp. Retinal damage was induced by injection (2 µl/eye) either of NMDA (Sigma-Aldrich) at 20 mM dissolved in 0.01 M phosphate-buffered saline (PBS) or of tunicamycin at 50 and 500 µg/ml, or (b) by acutely increasing the intraocular pressure (IOP). For NMDA- or tunicamycin-induced injury, the relevant agent was injected into the vitreous body of the left eye under the above anesthesia. In the IOP elevation model, the pupils were dilated with topical 2.5% phenylephrine hydrochloride and 1% tropicamide (Santen Pharmaceuticals Co. Ltd., Osaka, Japan). After topical instillation of 0.4% oxybuprocaine hydrochloride (Santen Pharmaceuticals Co. Ltd.), the anterior chamber was cannulated with a 32-gauge needle connected to a reservoir containing 0.9% NaCl. IOP was elevated by raising the height of the reservoir, maintaining a pressure of 100 mm Hg for 45 min. Retinal ischemia was confirmed by the blanching of the iris and retinal circulation. At the end of the elevated IOP period, the needle was removed, and reperfusion of the retinal vasculature was confirmed by ophthalmoscopic examination (KOM 300; Konan Inc., Nishinomiya, Japan). One drop of levofloxacin ophthalmic solution (Santen Pharmaceuticals Co. Ltd.) was applied topically to the treated eye after each procedure (intravitreal injection or ischemia-reperfusion).

Monitoring endoplasmic reticulum (ER) stress using ERAI-transgenic mice: In anesthetized ERAI-transgenic or wild-type mice, retinal damage was induced by injection (2 µl/eye) of either NMDA at 20 mM or tunicamycin at 50 µg/ml into the vitreous body, or by elevating IOP to 100 mmHg for 45 min (see above). Twenty-four hours later, the fluorescence intensity arising from the XBP-1-venus fusion protein, which is translated from the F-XBP1DDBD-venus gene, was visualized in the retina of anesthetized animals using an ophthalmoscope (TRC-50; TOPCON, Tokyo, Japan) fitted with a fluorescence filter. In separate experiments, the distribution and time-course of changes in fluorescence intensity in the retina were measured in retinal flatmount and cross-section specimens using either laser confocal microscopy (Bio-Lad Laboratories, Inc, Hercules, CA) or epifluorescence microscopy (Power BX50; Olympus, Tokyo, Japan). At various times after the intravitreal injections (12, 24, and 72 h), eyes were enucleated, then fixed in 4% paraformaldehyde for 1 h or overnight at 4 °C as preparation for retinal flatmount and retinal cross-section, respectively. For the preparation of retinal flatmounts, detached retinas were flatmounted on slides (MAS COAT; MATSUNAMI GLASS IND., LTD., Osaka, Japan) by making radial incisions. They were then mounted under a coverslip and observed using the epifluorescence microscope. For the preparation of retinal cross-sections, fixed eyes were immersed in 20% sucrose for 48 h at 4 °C, and embedded in optimum cutting temperature (OCT) compound (Sakura Finetechnical Co., Ltd, Tokyo, Japan). Transverse, 10 µm thick cryostat sections were cut and placed onto slides (MAS COAT) under a coverslip, and observed using the laser confocal microscope.

Immunoblotting: RGC-5 cells or mouse retinas were lysed using a cell-lysis buffer (RIPA buffer (R0278; Sigma) with protease (P8340; Sigma Aldrich) and phosphatase inhibitor cocktails (P2850 and P5726; Sigma), and 1 mM EDTA). Cell lysates were solubilized in SDS-sample buffer, separated on 10% SDS-polyacrylamide gels, and transferred to PVDF membrane (Immobilon-P; Millipore, Bedford, MA). Transfers were blocked for 1 h at room temperature with 5% Blocking One-P (Nakarai Tesque, Inc., Kyoto, Japan) in 10 mM Tris-buffered saline with 0.05% Tween 20 (TBS-T), then incubated overnight at 4 °C with the primary antibody. The transfers were then rinsed with TBS-T and incubated for 1 h at room temperature in horseradish peroxidase goat anti-rabbit or goat anti-mouse (Pierce, Rockford, IL) diluted 1:2000. The immunoblots were developed using chemiluminescence (Super Signal® West Femto Maximum Sensitivity Substrate; Pierce), and visualized with the aid of a digital imaging system (FAS-1000; Toyobo CO., LTD, Osaka, Japan). The primary antibodies used were as follows: mouse anti-BiP (BD Bioscience, San Jose, CA), rabbit anti-phospho-eIF2α (Ser51; Cell Signaling, Beverly, MA), rabbit anti-eIF2α (Cell Signaling), mouse anti-CHOP (Santa Cruz, Santa Cruz, CA), and rabbit anti-actin (Santa Cruz).

Immunostaining: To clarify the distribution and localization of the XBP1-venus fusion protein in the retina of ERAI mice (as seen in the retinal flatmounts and cross sections), double-staining immunocytochemistry was performed. At various times after intravitreal injections (12, 24, and 72 h), eyes were enucleated, fixed in 4% paraformaldehyde overnight at 4 °C, immersed in 20% sucrose for 48 h at 4 °C, and embedded in optimum cutting temperature (OCT) compound (Sakura Finetechnical Co., Ltd, Tokyo, Japan). Transverse, 10 µm thick cryostat sections were cut and placed onto slides MAS COAT (MATSUNAMI GLASS IND., LTD.). Sections were subsequently processed for immunocytochemical localization using antibodies against CHOP (1:100 dilution in PBS; Santa Cruz), glucose-regulated protein 78(GRP78)/BiP (1:100 dilution in PBS), thymus cell antigen 1 (Thy-1; 1:100 dilution in PBS; Serotec Ltd, Oxford UK), microglia (OX-42, 1:100 dilution in PBS; Serotec Ltd), and amacrine cells (HPC-1/Syntaxin, 1:100 dilution in PBS; Santa Cruz). The sections were incubated either (a) with Alexa Fluor-568-conjugated secondary antibody (1:200 dilution in PBS; Molecular Probes, Eugene, OR) for 1 h at room temperature, mounted with a coverslip, and observed under a laser confocal microscope (Bio-Lad Laboratories, Inc), or (b) with biotin-conjugated secondary antibody for 1 h at room temperature, and visualized using a VECTOR M.O.M. Immunodetection kit (Vector, Burlingame, CA). Each image was taken using a digital camera (Coolpix 4500; Nikon, Tokyo, Japan) attached with epifluorescence microscope (Power BX50; Olympus).

Histological analysis of mouse retina: Seven days after the NMDA or tunicamycin injection, eyeballs were enucleated for histological analysis. In mice under anesthesia, produced by an intraperitoneal injection of sodium pentobarbital (80 mg/kg), each eye was enucleated, then kept immersed for at least 24 h at 4 °C in a fixative solution containing 4% paraformaldehyde. Six paraffin-embedded sections (thickness, 3 µm) cut through the optic disc of each eye were prepared in a standard manner, and stained with hematoxylin and eosin. Retinal damage was evaluated as described previously, and three sections from each eye were used for the morphometric analysis. Light-microscope photographs were taken using a digital camera (Coolpix 4500, Nikon) and the cell counts in the ganglion cell layer (GCL) and the thickness of the inner plexiform layer (IPL) at a distance between 350 and 650 µm from the optic disc were measured on the images in a masked fashion by a single observer (Y.I.). Data from three sections (selected randomly from the six sections) were averaged for each eye, and the values obtained were used to evaluate the GCL cell count and the IPL thickness.

Statistical analysis: Data are presented as the means±SEM. Statistical comparisons were made using a Student's *t*-test or Dunnett's test, by means of STAT VIEW version 5.0 (SAS Institute Inc., Cary, NC). $P<0.05$ was considered to be statistically significance.

RESULTS

Retinal cell death and time-course of changes in endoplasmic reticulum (ER) stress-related protein induced by tunicamycin: We examined whether tunicamycin treatment could induce cell death through ER stress in retinal ganglion cell using RGC-5. Representative fluorescence stainings of nuclei [using Hoechst 33342, YO-PRO-1, and propidium iodide (PI) dyes] are shown in Figure 1A. Vehicle-treated control cells displayed normal nuclear morphology and negative staining with both YO-PRO-1 dye (which stains early apoptotic and later-stage cells) and PI dye (which stains late-stage apoptotic cells; upper panels in Figure 1A). Treatment with tunicamycin led to shrinkage and condensation of nuclei, and to positive staining with each of these dyes (lower panels in Figure 1A). The number of cells exhibiting PI fluorescence was counted, and positive cells were expressed as the percentage of PI- to Hoechst 33342-positive cells (Figure 1B). After treatment with tunicamycin at 1, 2, or 4 µg/ml for 24 h, the percentages of PI-positive cells were 8.3±1.2% (n=6), 13.1±0.9% (n=6), and 11.3±0.6% (n=6), respectively, while in the non-treated control group the percentage was 0.5±0.2% (n=6). After treatment with tunicamycin at 1, 2, or 4 µg/ml for a longer time period (48 h), the corresponding values were 41.5±3.5% (n=6), 43.7±2.1% (n=6), and 50.7±2.6% (n=6), respectively (1.2±0.4% (n=6) for the non-treated control group). Time-course data for the changes in the protein levels of glucose-regulated protein (GRP)78/BiP, the phosphorylated form of eukaryotic initiation factor 2α (eIF2α), total eIF2α, and C/EBP-homologous protein (CHOP) occurring after tunicamycin treatment at 2 µg/ml are shown in Figure 1C. BiP, a biomarker of ER-stress, increased time-dependently throughout the 24 h tunicamycin treatment period, while actin levels remained unchanged. Treatment with tunicamycin time-dependently induced eIF2α phosphorylation, while total eIF2α levels were not changed during the 24 h observation period. CHOP was first detected at 6 h after addition of tunicamycin and persisted thereafter. These data indicate that treatment with tunicamycin can induce expres-

sions of ER stress-related proteins and subsequent apoptotic cell death in RGC-5 culture in vitro.

Intravitreal injection of tunicamycin induces retinal cell death in mice: To clarify whether tunicamycin would induce retinal cell death in vivo, we examined the histological changes in the retina at 7 days after intravitreal injection of tunicamycin. As shown in Figure 2, intravitreal injection of tunicamycin at 0.1 μg/eye (a low dose) induced a significant loss of cells in the retinal ganglion cell layer (GCL), but no thinning of the inner plexiform layer (IPL; versus vehicle-treated retinas). At a high dose of 1μg/eye, tunicamycin significantly decreased both the cell count in GCL and the IPL thickness (versus the non-treated normal retina; Figure 2). On the other hand, no retinal damage was induced by intravitreal injection of an identical volume of vehicle (versus the non-treated retina). Together, these findings suggest that tunicamycin at 0.1 μg/eye (giving an estimated concentration in the vitreous body of approximately 10 μg/ml) induces retinal ganglion cell death at a concentration similar to that inducing exhibiting the apoptotic cell death in RGC-5 in vitro.

Increase in XBP-1-venus fusion protein in the retina in ER stress-activated indicator (ERAI)-transgenic mice: To investigate whether ER stress is induced in the mouse retina during the early stages of retinal damage in vivo, we used ERAI-transgenic mice carrying the F-XBP1DDBD-venus expression gene, which allows effective identification of cells under ER stress in vivo, as previously described by Iwawaki et al. [11]. Twenty-four h after intravitreal injection of tunicamycin at 0.1 μg or of *N*-methyl-D-aspartate (NMDA) at 40 nmol, the fluorescence intensity arising from the XBP-1-venus fusion protein was visualized in the retina of anesthetized animals (using an ophthalmoscope) as shown in Figure 3. Both tunicamycin and NMDA increased the fluorescence intensity of this protein, while little change in fluorescence intensity was observed in the control fellow eyes. For further elucidation of this phenomenon, the distribution and time-course of changes in the fluorescence intensity derived from the XBP-1-venus fusion protein were measured in retinal flatmount and transverse sections, as shown in Figure 4A,C. In the flatmounts, such stimulations as NMDA, an intraocular

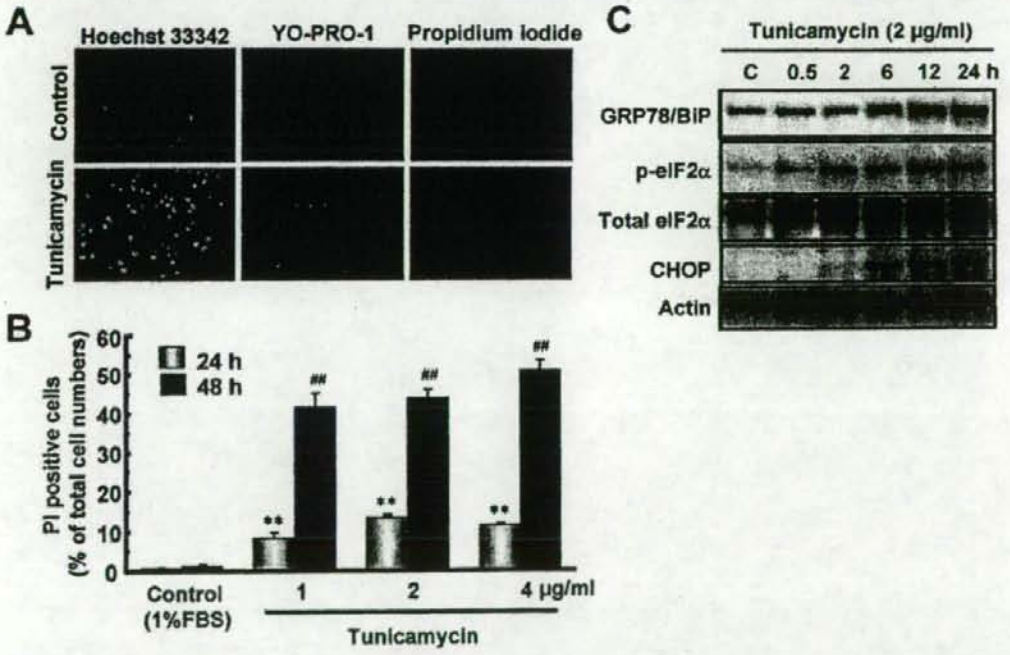

Figure 1. Retinal cell death and time-course of changes in endoplasmic reticulum (ER)-stress related proteins induced by tunicamycin. A: Representative fluorescence microscopy showing nuclear stainings for Hoechst 33342 (blue), YO-PRO-1 (green), and propidium iodide (PI, red) at 48 h after addition of tunicamycin at 1 μg/ml. B: The number of cells displaying PI fluorescence was counted at two time-points, and positive cells were expressed as the percentage of PI to Hoechst 33342. Each column represents the mean±SEM (n=6). Double asterisks and double hash marks; $p<0.01$ versus corresponding control group (Dunnett's test). C: Representative immunoblots showing the time-course of changes in protein levels (GRP78/BiP, phosphorylated-eIF2α, total eIF2α, and CHOP) after tunicamycin treatment at 2 μg/ml.

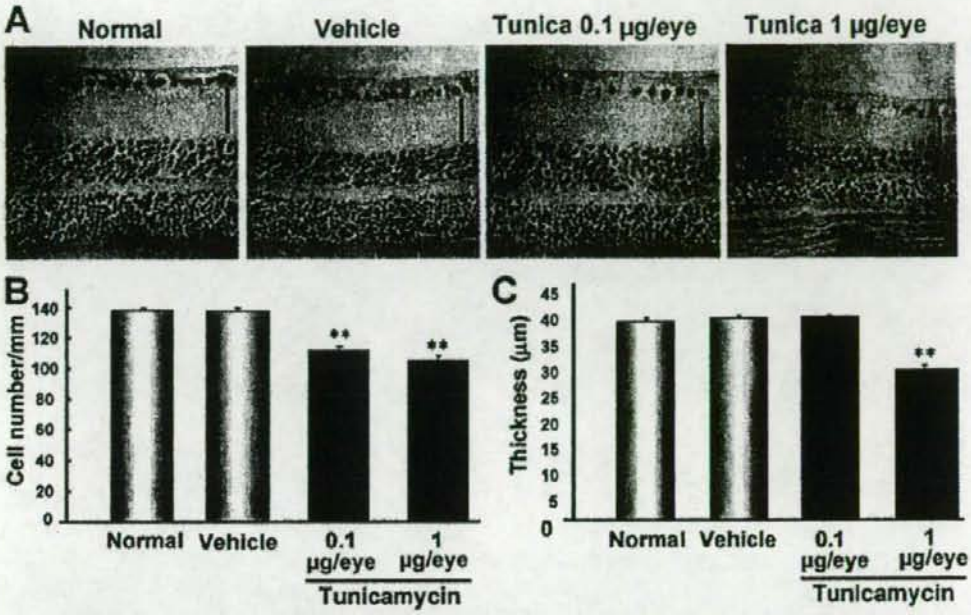

Figure 2. Intravitreal injection of tunicamycin induces retinal cell death in mice. A: Representative photographs showing non-treated normal retina, vehicle-treated retina, and low-dose (0.1 µg/eye) and high-dose (1 µg/eye) tunicamycin-treated retinas 7 days after intravitreal injection. Quantitative analysis of cell number in ganglion cell layer (B) and thickness of inner plexiform layer (IPL) C: Each column represents the mean±SEM (n=10). Double asterisks $p<0.01$ versus vehicle-treated control group (Dunnett's test). The horizontal scale bar represents 25 µm and the vertical bar indicates each thickness of IPL.

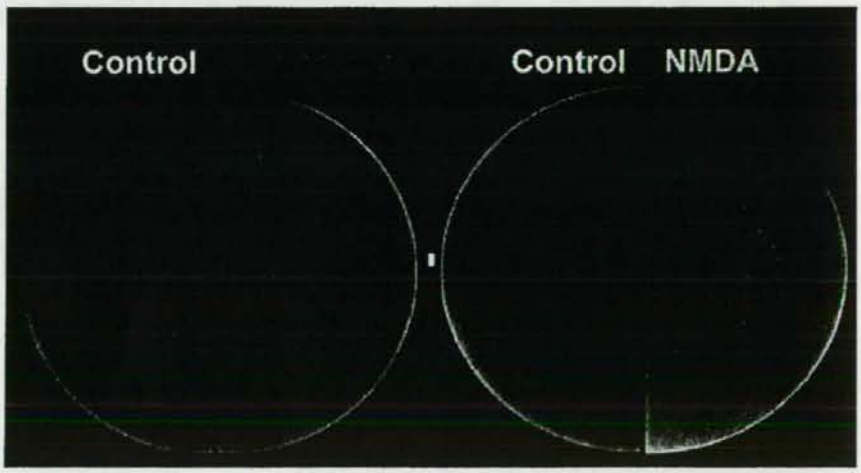

Figure 3. Non-invasive imaging of XBP-1-venus fusion protein in ERAI mouse retina in vivo. Twenty-four hours after intravitreal injection of either tunicamycin at 0.1 µg/eye or *N*-methyl-D-aspartate (NMDA) at 40 nmol/eye, the fluorescence intensity arising from XBP-1-venus fusion protein was visualized in the retinas of anesthetized animals using an ophthalmoscope fitted with a fluorescence filter.

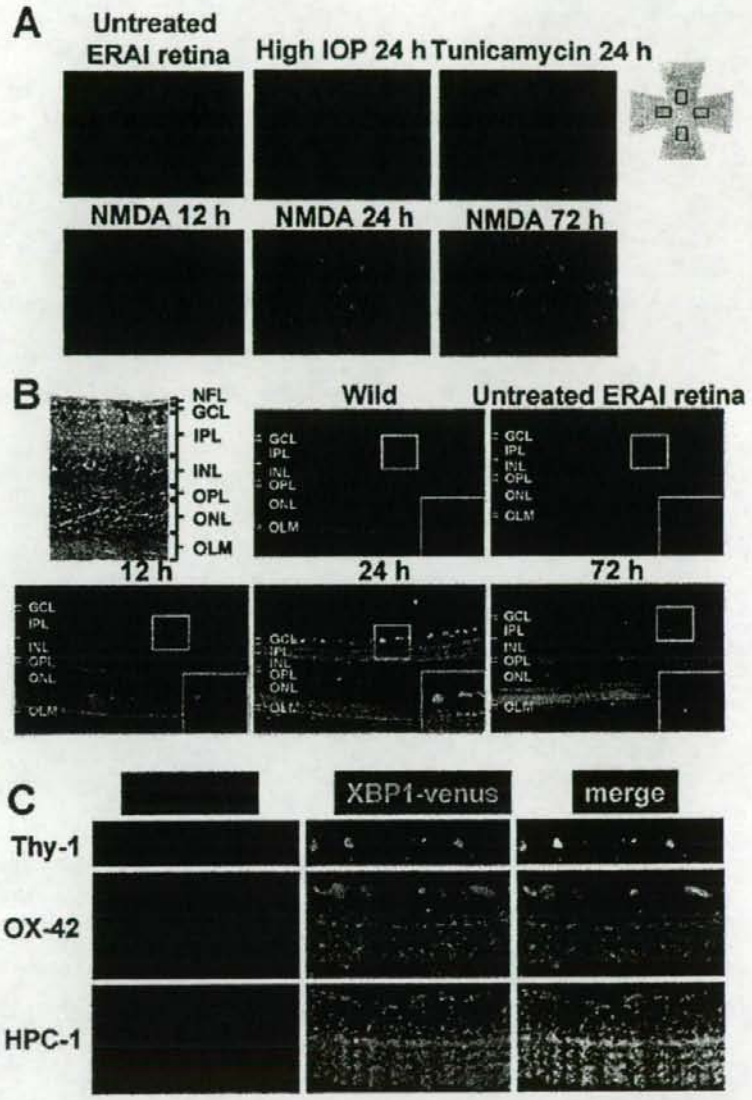

Figure 4. Expression and localization of XBP-1-venus fusion protein in ERAI mouse retinas after various types of retinal damage. **A**: Representative fluorescence photographs of increased XBP-1-venus fusion protein in ERAI mouse flatmounted retina after *N*-methyl-D-aspartate (NMDA), intraocular pressure (IOP) elevation, or tunicamycin insult. The fluorescence (green) arising from XBP-1-venus fusion protein was observed under an epifluorescence microscope. The scale bar represents 25 µm. **B**: Distribution of increased XBP-1-venus fusion protein in retinal cross-sections from ERAI mice after NMDA injection at 40 nmol/eye. The distribution of fluorescence (green) arising from XBP-1-venus fusion protein was observed under a laser confocal microscope. Each large box shows an enlargement of the area within the corresponding small box. **C**: Localization of XBP-1-venus fusion protein in ERAI mouse retina after NMDA injection. In the retinal nerve fiber layer (upper panels), Thy-1-positive cells (red) can be seen to merge with XBP-1-venus fusion protein (green). In the middle panels, OX-42 (a microglia marker)-positive cells (red) are partly merged with XBP-1-venus fusion protein (green). In the inner plexiform layer (lower panels), HPC-1 (an amacrine marker)-positive cells (red) are merged with XBP-1-venus fusion protein (green).

pressure (IOP) elevation, and tunicamycin all induced increases in fluorescence intensity at the time-points indicated in Figure 4A. In the NMDA-treated retinas of ERAI mice, the background fluorescence intensity was time-dependently increased in the period from 12 to 72 h, but little change was observed in the NMDA-treated retinas of wild-type mice.

These changes in background could reflect increases in the lower part of the ganglion cell layer, such as the inner plexiform layer and neuroepithelial layer, of the retina. In transverse sections, increases in fluorescence intensity were first observed in cells of the GCL and inner plexiform layer at 12 and 24 h, respectively, after NMDA injection, and the increases peaked in GCL cells at 24 h (Figure 4B). The increase in fluorescence had diminished at 72 h after the NMDA injection, but morphologically distinct cells (such as microglia cells) had appeared in GCL. On the other hand, the retinas of wild-type and non-treated ERAI mice showed a low fluorescence intensity (below background), while a slight fluorescence intensity was observed in the neuroepithelial layer of the retina (Figure 4B). These cells merged with Thy-1-positive cells (ganglion cells) and some OX-42-positive cells (microglia) in GCL, and with HPC-1-positive cells (amacrine cells) in IPL (Figure 4C). Together, these results suggest that XBP-1 splicing, representing activation of the ER-stress signal pathway, may be induced in retinal ganglion and amacrine and microglia cells during the early stages of retinal cell damage.

Increases in GRP78/BiP and CHOP in mouse retina after NMDA injection: To clarify whether ER stress-related proteins other than XBP-1 are induced in the mouse retina by NMDA stimulation, we examined the changes in BiP, a biomarker of ER stress, in the retina after intravitreal injection of NMDA. As shown in Figure 5B, cell loss in GCL and thinning of IPL were observed at 72 h after NMDA injection (versus non-treated control retinas; Figure 5A). Using immunoblots, as shown in Figure 5C, we found that BiP was significantly increased at 12 h after the NMDA injection, and that the increase persisted for the remainder of the 72 h observation period. Next, we investigated the distribution and time-course of changes in GRP78/BiP and CHOP, a proapoptosis protein, after NMDA injection. In the non-treated control retina, slight immunoreactivities for BiP and CHOP were observed in a number of cells in GCL and IPL (Figure 5D). Increases in these immunoreactivities were observed in retinal ganglion cells at 12 h after NMDA injection, and time-dependent increases were noted in the inner retina (Figure 5D).

DISCUSSION

In the present study, we could detect pathological changes and time-dependent changes related to ER stress in retinal flatmount and transverse sections and in the retinas of living mice after retinal damage. Moreover, we demonstrated that ER stress signals were activated in the retina in vivo after tunicamycin, elevating IOP, or NMDA treatment.

Agents or conditions that adversely affect ER protein folding lead to an accumulation of unfolded or misfolded proteins in the ER, a condition defined as ER stress. ER stress can be induced by agents or conditions that interfere with (a) protein glycosylation (e.g., glucose starvation, tunicamycin, glucosamine), (b) disulfide-bond formation (e.g., DTT, homocysteine), (c) Ca^{2+} balance (A23187, thapsigargin, EGTA), and/or (d) a general overloading of the ER with proteins (e.g., viral or non-viral oncogenesis) [1,13,14]. However, little is known about any involvement of ER stress in retinal damage. In the present study, we found that tunicamycin induced the ER stress-associated proteins BiP, p-eIF2α, and CHOP in cultured RGC-5 cells. These protein levels started to increase at 2 to 6 h after the start of tunicamycin treatment, and increased time-dependently until 24 h after the start of the treatment, while apoptotic cell death with condensation and fragmentation of nuclei was observed 24 h later. BiP acts as an ER resident molecular chaperon that is induced by ER stress, and this protein refolds the unfolded proteins, thereby tending to maintain homeostasis in the ER [15,16]. Since CHOP is a member of the CCAAT/enhancer-binding protein family that is induced by ER stress and participates in ER-mediated apoptosis, CHOP may be a key molecule in retinal cell death [17]. In the present study, the phosphorylation of eIF2α was increased concomitantly with the increases in the expression of BiP and CHOP proteins, even through p-eIF2α might be expected to suppress protein synthesis. Boyce et al.[18] reported that selective inhibition of eIF2α dephosphorylation increases both p-eIF2α and CHOP protein. These data suggest that during ER stress, p-eIF2α (inactive form) is still able to stimulate the translation of ATF4 mRNA, thereby increasing the transcription of BiP or CHOP mRNA, but that enough unphosphorylated-eIF2α (active form) may remain to translate BiP and CHOP mRNAs to proteins. On the other hand, we found that staurosporine, which mediates mitochondrial dysfunctions resulting in apoptotic cell death, did not induce any increases in BiP and CHOP proteins in RGC-5 [unpublished data]. Taken together, these findings suggest that persistent ER stress may induce apoptotic cell death through the eIF2α-CHOP signal pathway in RGC-5.

Next, we tried to determine whether tunicamycin could induce retinal damage in vivo. Intravitreal injection of low-dose tunicamycin induced a significant loss of cells in the retinal ganglion cell layer (GCL), but no thinning of the inner plexiform layer (IPL). These findings suggest that retinal ganglion cells are more sensitive to ER stress-induced cell death than other retinal cells. High-dose tunicamycin significantly decreased both the cell count in GCL and the thickness of IPL. The concentration of tunicamycin in the vitreous body after an intravitreal injection of low-dose tunicamycin was estimated to be 10 μg/ml. The tunicamycin concentration achieved within the retina will have been less than this. Interestingly, in the present in vitro study, tunicamycin at 1 to 4 μg/ml induced cell death with an increase in ER-stress signals, suggesting that the in vivo concentration of tunicamycin in the retina was roughly similar to that employed in vitro. Use of tunicamycin at a high dose also led to decreases in IPL, INL (inner nuclear layer), and ONL (outer nuclear layer) in the retina. In guinea pigs, a single subcutaneous injection of tunicamycin at 0.4 mg/kg has been reported to induce hepatotoxicity with dilation of the cisternae of the ER [19]. Fur-

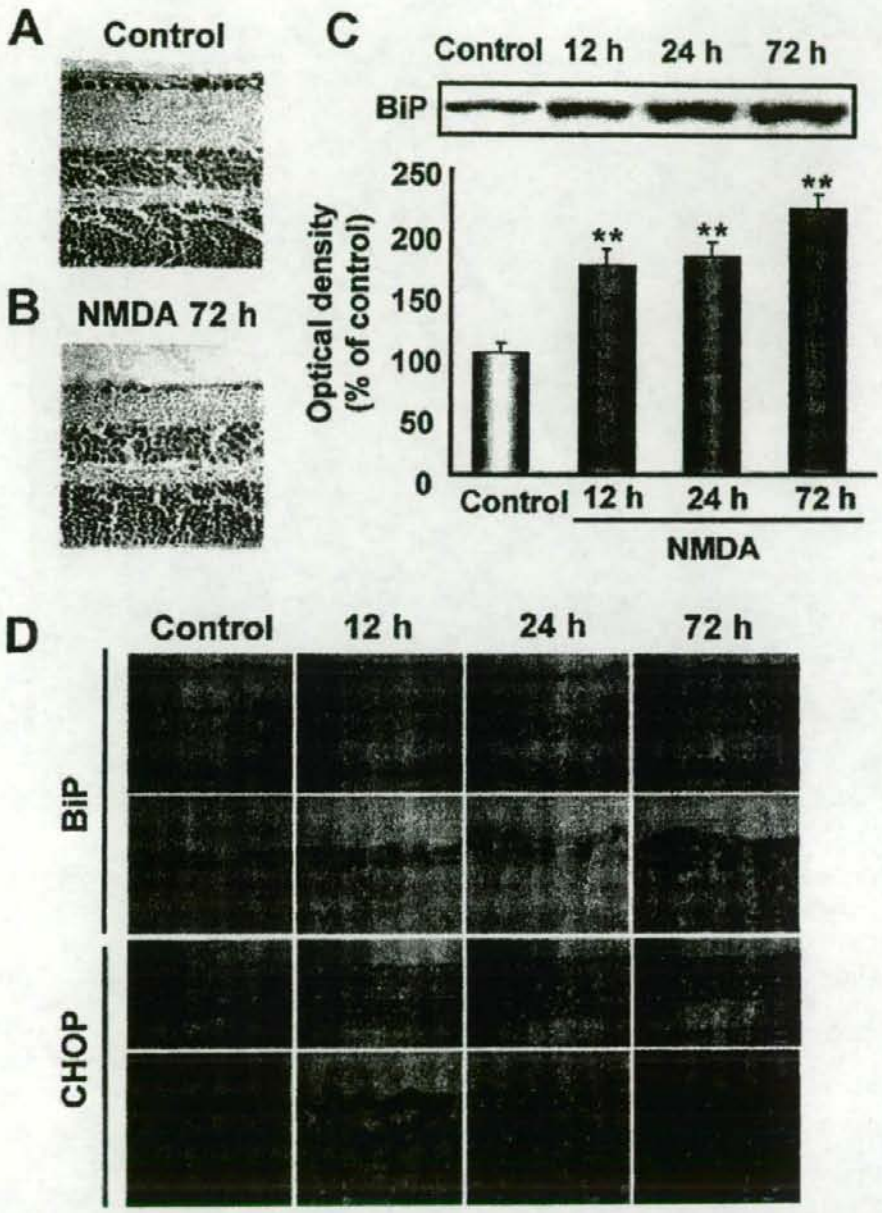

Figure 5. Increases in GRP78/BiP and CHOP in retinal extracts following stimulation by intravitreal injection of *N*-methyl-D-aspartate (NMDA) in mice. **A, B**: Representative photographs showing retinal cross-sections stained with hematoxylin and eosin after NMDA injection at 40 nmol/eye. **C**, upper panel: Representative immunoblots showing the time-course of changes in GRP78/BiP protein levels after intravitreal injection of NMDA. **C**, lower panel: Quantitative analysis of GRP78/BiP band densities. Data are expressed as mean±SEM (n=6) of values (in arbitrary units) obtained for single band density. Double asterisks represents $p<0.01$ versus vehicle-treated control group (Dunnett's test). **D**: Immunostainings for GRP78/BiP and CHOP in mouse retina after NMDA injection at 40 nmol. The scale bar represents 25 μm.

thermore, Zinszner et al.[20] noted that in mice, a single sublethal intraperitoneal injection of tunicamycin (1 mg/kg) induces CHOP expression and subsequent severe histological damage with an increase in TUNEL-positive cells, and a characteristic transient renal insufficiency. They also found that CHOP-deficient mice show an attenuated increase in TdT-mediated dUTP nick-end labeling (TUNEL)-positive cells during the renal damage induced by tunicamycin. These findings suggest that in vivo, tunicamycin-induced retinal cell death is due, at least in part, to an ER-stress mechanism.

NMDA receptors may participate in the processes of excitotoxicity and neuronal death in the retina [21,22]. Previous studies have found that TUNEL-positive cells can be observed in the GCL and INL of the mouse retina at an early stage (within 24 h) after an intravitreal injection of NMDA [23,24]. The hallmark of NMDA-induced neuronal death is a sustained increase in the intracellular Ca^{2+} concentration accompanied by overactivation of vital Ca^{2+}-dependent cellular enzymes [25]. Thus, the signal-transduction pathways for NMDA-mediated cell death in the retina are well studied, but not yet fully understood.

To illuminate the role and distribution of ER stress in vivo, we focused on the retina of ERAI mice. Information about the status of ER stress during the course of a given disease might be obtained by crossing an ERAI transgenic mouse (the indicator mouse for ER stress in living cells) with a mouse model of the human disease of interest. In flatmounted retinas, fluorescence was detected following various stimulations [tunicamycin, NMDA, and intraocular pressure (IOP) elevation]. To our knowledge, this is the first report demonstrating that NMDA and ischemic insult (elevating IOP), in addition to tunicamycin, can activate the ER stress signal (measured as the splicing of the XBP-1 and venus fusion gene in ERAI transgenic mice) in the retina in vivo. Interestingly, ER stress was also induced in the retina after a transient IOP elevation, defined as an ischemia-reperfusion model. It has been reported that this model exhibits retinal cell damage similar to that induced by NMDA, and that both of these examples of damage are protected against by MK-801, an NMDA receptor antagonist, and by NO synthetase-inhibitor treatment [8,26]. Although little is known about the precise mechanisms responsible for activation of ER stress after NMDA or IOP elevation (ischemia-reperfusion), both stimuli cause intracellular Ca^{2+} overload and increased NO production, resulting in apoptotic cell death. Several lines of study suggest that intracellular Ca^{2+} overload and excessive production of NO deplete Ca^{2+} in the ER, thereby resulting in ER stress [27,28]. Recently, Uehara et al.[10] reported that NO induces S-nitrosylation of protein-disulphide isomerase (PDI), an enzyme that assists in the maturation and transport of unfolded secretory proteins and thereby helps to prevent the neurotoxicity associated with ER stress. S-nitrosylated-PDI exhibits reduced enzymatic activity and induces cell death through the ER stress pathway. These mechanisms may contribute to the activation of ER stress in the retina after NMDA stimulation or IOP elevation. Accordingly, our findings may provide important new insights into the mechanisms underlying the retinal cell damage induced by NMDA and by ischemia-reperfusion. In transverse retinal sections, we observed an increase in fluorescence intensity within the cells of the ganglion cell layer (GCL) and inner plexiform layer (IPL) at 12 and 24 h, respectively, after NMDA injection. The cells displaying increased fluorescence were ganglion cells (at 12 h after the injection), amacrine cells in IPL (at 24 h), and microglia in GCL (at 72 h). These data indicate that ganglion cells may be more sensitive to ER stress than the other retinal cells examined.

To further clarify the participation of ER stress, we examined the changes in BiP and CHOP in the retina after NMDA-induced injury. We found (a) that NMDA induced BiP proteins in the retina at 12 h after its injection (on the basis of immunoblots), and (b) that, NMDA induced both BiP and CHOP in the retina (especially within retinal ganglion cells and INL) at 12 h after its injection (on the basis of our immunostaining results). The expression of the CHOP gene reportedly increases in the rat retina after intravitreal injection of NMDA [29]. Furthermore, Awai et al.[30] found that treatment with MK-801, an NMDA receptor antagonist, inhibited the increases in CHOP mRNA and protein in the mouse retina that are observed after intravitreal injection of NMDA, and moreover that CHOP-deficient mice were resistant to NMDA-induced retinal damage. However, CHOP-deficient mice partially suppressed the NMDA-induced cell death, and therefore other pathways, such as mitochondrial dysfunction, may be engaged in the retinal cell death. Collectively, the above results indicate that NMDA can cause ER stress in the retina, and that the neurotoxicity induced by NMDA is due in part to a mechanism dependent on CHOP protein induction through excessive ER stress.

In conclusion, we have identified a close association between ER stress and retinal damage, and our results suggest that the ER stress-signal pathway might be a good target in the treatment of retinal diseases.

ACKNOWLEDGEMENTS

This study was supported by a donation from the late Emeritus Professor Akihide Koda (Gifu Pharmaceutical University), for which we are very grateful. This work was supported in part by research grants from a Grant-in-Aid for scientific research from the Ministry of Education, Culture, Sports, Science, and Technology, Japan, the Gifu Research and Development Foundation, the Ministry of Education, Science, Sports, Culture of the Japanese Government (No.17591848), and the Naito Foundation.

The authors wish to express their gratitude to Dr. Neeraj Agarwal, Department of Pathology and Anatomy, UNT Health Science Center, Forth Worth, TX, USA, for the kind gift of RGC-5, and to Mr. Yasuhisa Oida and Mr. Nobutaka Morimoto for skillful technical assistance.

REFERENCES

1. Kaufman RJ. Stress signaling from the lumen of the endoplasmic reticulum: coordination of gene transcriptional and translational controls. Genes Dev 1999; 13:1211-33.
2. Harding HP, Calfon M, Urano F, Novoa I, Ron D. Transcriptional

and translational control in the Mammalian unfolded protein response. Annu Rev Cell Dev Biol 2002; 18:575-99.
3. Aridor M, Balch WE. Integration of endoplasmic reticulum signaling in health and disease. Nat Med 1999; 5:745-51.
4. Bonne C, Muller A, Villain M. Free radicals in retinal ischemia. Gen Pharmacol 1998; 30:275-80.
5. Dreyer EB. A proposed role for excitotoxicity in glaucoma. J Glaucoma 1998; 7:62-7.
6. Neufeld AH. Nitric oxide: a potential mediator of retinal ganglion cell damage in glaucoma. Surv Ophthalmol 1999; 43 Suppl 1:S129-35.
7. McKinnon SJ. Glaucoma, apoptosis, and neuroprotection. Curr Opin Ophthalmol 1997; 8:28-37.
8. Adachi K, Kashii S, Masai H, Ueda M, Morizane C, Kaneda K, Kume T, Akaike A, Honda Y. Mechanism of the pathogenesis of glutamate neurotoxicity in retinal ischemia. Graefes Arch Clin Exp Ophthalmol 1998; 236:766-74.
9. Sucher NJ, Lipton SA, Dreyer EB. Molecular basis of glutamate toxicity in retinal ganglion cells. Vision Res 1997; 37:3483-93.
10. Uehara T, Nakamura T, Yao D, Shi ZQ, Gu Z, Ma Y, Masliah E, Nomura Y, Lipton SA. S-nitrosylated protein-disulphide isomerase links protein misfolding to neurodegeneration. Nature 2006; 441:513-7.
11. Iwawaki T, Akai R, Kohno K, Miura M. A transgenic mouse model for monitoring endoplasmic reticulum stress. Nat Med 2004; 10:98-102.
12. Krishnamoorthy RR, Agarwal P, Prasanna G, Vopat K, Lambert W, Sheedlo HJ, Pang IH, Shade D, Wordinger RJ, Yorio T, Clark AF, Agarwal N. Characterization of a transformed rat retinal ganglion cell line. Brain Res Mol Brain Res 2001; 86:1-12.
13. Pahl HL. Signal transduction from the endoplasmic reticulum to the cell nucleus. Physiol Rev 1999; 79:683-701.
14. Lee AS. The glucose-regulated proteins: stress induction and clinical applications. Trends Biochem Sci 2001; 26:504-10.
15. Kleizen B, Braakman I. Protein folding and quality control in the endoplasmic reticulum. Curr Opin Cell Biol 2004; 16:343-9. Erratum in: Curr Opin Cell Biol 2004; 16:597.
16. Gething MJ. Role and regulation of the ER chaperone BiP. Semin Cell Dev Biol 1999; 10:465-72.
17. Oyadomari S, Mori M. Roles of CHOP/GADD153 in endoplasmic reticulum stress. Cell Death Differ 2004; 11:381-9.
18. Boyce M, Bryant KF, Jousse C, Long K, Harding HP, Scheuner D, Kaufman RJ, Ma D, Coen DM, Ron D, Yuan J. A selective inhibitor of eIF2α dephosphorylation protects cells from ER stress. Science 2005; 307:935-9.
19. Finnie JW, O'Shea JD. Acute hepatotoxicity with resultant pulmonary and cerebral embolism in guinea pigs given tunicamycin. Pathology 1989; 21:194-9.
20. Zinszner H, Kuroda M, Wang X, Batchvarova N, Lightfoot RT, Remotti H, Stevens JL, Ron D. CHOP is implicated in programmed cell death in response to impaired function of the endoplasmic reticulum. Genes Dev 1998; 12:982-95.
21. Sabel BA, Sautter J, Stoehr T, Siliprandi R. A behavioral model of excitotoxicity: retinal degeneration, loss of vision, and subsequent recovery after intraocular NMDA administration in adult rats. Exp Brain Res 1995; 106:93-105.
22. Siliprandi R, Canella R, Carmignoto G, Schiavo N, Zanellato A, Zanoni R, Vantini G. N-methyl-D-aspartate-induced neurotoxicity in the adult rat retina. Vis Neurosci 1992; 8:567-73.
23. Hara A, Niwa M, Kumada M, Kitaori N, Yamamoto T, Kozawa O, Mori H. Fragmented DNA transport in dendrites of retinal neurons during apoptotic cell death. Brain Res 2004; 1007:183-7.
24. Li Y, Schlamp CL, Nickells RW. Experimental induction of retinal ganglion cell death in adult mice. Invest Ophthalmol Vis Sci 1999; 40:1004-8.
25. Fukunaga K, Soderling TR, Miyamoto E. Activation of Ca2+/calmodulin-dependent protein kinase II and protein kinase C by glutamate in cultured rat hippocampal neurons. J Biol Chem 1992; 267:22527-33.
26. Lam TT, Siew E, Chu R, Tso MO. Ameliorative effect of MK-801 on retinal ischemia. J Ocul Pharmacol Ther 1997; 13:129-37.
27. Li WW, Alexandre S, Cao X, Lee AS. Transactivation of the grp78 promoter by Ca2+ depletion. A comparative analysis with A23187 and the endoplasmic reticulum Ca(2+)-ATPase inhibitor thapsigargin. J Biol Chem 1993; 268:12003-9.
28. Oyadomari S, Araki E, Mori M. Endoplasmic reticulum stress-mediated apoptosis in pancreatic beta-cells. Apoptosis 2002; 7:335-45.
29. Laabich A, Li G, Cooper NG. Characterization of apoptosis-genes associated with NMDA mediated cell death in the adult rat retina. Brain Res Mol Brain Res 2001; 91:34-42.
30. Awai M, Koga T, Inomata Y, Oyadomari S, Gotoh T, Mori M, Tanihara H. NMDA-induced retinal injury is mediated by an endoplasmic reticulum stress-related protein, CHOP/GADD153. J Neurochem 2006; 96:43-52.

The print version of this article was created on 5 Apr 2007. This reflects all typographical corrections and errata to the article through that date. Details of any changes may be found in the online version of the article.

Involvement of Double-Stranded RNA-Dependent Protein Kinase in ER Stress-Induced Retinal Neuron Damage

Masamitsu Shimazawa, Yasushi Ito, Yuta Inokuchi, and Hideaki Hara

Purpose. To clarify whether the activation of double-stranded RNA-dependent protein kinase (PKR) participates in the cell death induced by endoplasmic reticulum (ER) stress, the authors used cultured retinal ganglion cells (RGC-5, a rat ganglion cell line transformed with the E1A virus) in vitro and the effect of a PKR inhibitor (an imidazolo-oxindole derivative) on *N*-methyl-D-aspartate (NMDA)–induced retinal damage in mice in vivo.

Methods. In RGC-5 culture, cell damage was induced by tunicamycin (an ER stress inducer), and cell viability was measured by Hoechst 33342, YO-PRO-1, or propidium iodide (PI) double staining or by the resazurin-reduction test. Levels of glucose-regulated protein (GRP) 78/BiP, activating transcription factor 4 (ATF4), C/EBP-homologous protein (CHOP) and the phosphorylated form of PKR were analyzed by immunoblot. The PKR inhibitor and two siRNAs that recognize nonoverlapping sequences of rat PKR were tested for their effects on tunicamycin-induced cell death. In vivo, retinal cell damage was induced by intravitreal injection of NMDA (20 nmol/eye) in mice. To examine its effect in vivo, the PKR inhibitor (1 nmol/eye) was intravitreally injected with NMDA, and ganglion cell layer cell loss and inner plexiform layer thinning were evaluated 7 days after NMDA injection.

Results. Treatment with tunicamycin at 1, 2, and 4 μg/mL for 24 hours increased the number of YO-PRO-1 and PI-positive (apoptosis or necrosis indicator) cells in a concentration-dependent manner. Immunoblotting analysis showed that tunicamycin at 2 μg/mL induced BiP, ATF4, and CHOP protein production and PKR phosphorylation. Both the PKR inhibitor (0.03–1 μM) and the PKR knockdown (using siRNA) inhibited tunicamycin-induced RGC-5 cell death. The same inhibitor also reduced NMDA-induced retinal damage in vivo. The PKR inhibitor reduced the tunicamycin-induced increase in CHOP but not that in BiP protein production.

Conclusions. These results indicate that inhibiting PKR activation is neuroprotective against ER stress-induced retinal damage, suggesting that PKR activation may be involved in the mechanisms underlying ER stress-induced cell death. (*Invest Ophthalmol Vis Sci.* 2007;48:3729–3736) DOI:10.1167/iovs.06-1122

From the Department of Biofunctional Molecules, Gifu Pharmaceutical University, Gifu, Japan.

Supported by a donation from the late Emeritus Professor Akihide Koda and by a research grant from the Ministry of Education, Science, Sports, Culture of Japanese Government (Grant 17591848).

Submitted for publication September 19, 2006; revised February 14 and March 19, 2007; accepted June 12, 2007.

Disclosure: **M. Shimazawa**, None; **Y. Ito**, None; **Y. Inokuchi**, None; **H. Hara**, None

The publication costs of this article were defrayed in part by page charge payment. This article must therefore be marked "*advertisement*" in accordance with 18 U.S.C. §1734 solely to indicate this fact.

Corresponding author: Hideaki Hara, Department of Biofunctional Molecules, Gifu Pharmaceutical University, 5-6-1 Mitahora-higashi, Gifu 502-8585, Japan; hidehara@gifu-pu.ac.jp.

Endoplasmic reticulum (ER) stress has recently been linked to the pathogenesis of several diseases, including vascular and neurodegenerative diseases such as stroke, Alzheimer disease, and Parkinson disease.[1–3] Little is known about any role of ER stress in retinal damage.

Retinal ganglion cell (RGC) death is a common feature of many ophthalmic disorders, such as glaucoma, optic neuropathies, and of various retinovascular diseases (diabetic retinopathy, retinal vein occlusions). A variety of factors, including oxidative stress,[4] excitatory amino acids,[5] and nitric oxide,[6] have been reported to induce retinal cell death. These reports emphasize the importance of a better understanding of the precise mechanisms underlying retinal diseases.

Recently, it has been reported that one of the proapoptotic proteins involved in ER stress-mediated apoptosis (tunicamycin-induced apoptosis) is a double-stranded RNA-dependent protein kinase (PKR), as identified using a randomized ribozyme library.[7] PKR, an interferon-induced protein kinase identified initially in a study of responses to viral infection, is activated by the extensive secondary structure of viral RNA.[8] On binding to double-stranded RNA, PKR is autophosphorylated, and it then increases the cellular sensitivity to apoptotic stimuli through a number of putative pathways, including the phosphorylation of eukaryotic initiation factor 2α (p-eIF2α).[9,10] Thus, PKR is involved in the apoptosis induced not only by viral infection but also by ER stress. Hence, the purpose of the present study was to examine whether a PKR inhibitor (an imidazolo-oxindole derivative that acts as an ATP-binding site-directed inhibitor of PKR) or PKR silencing (by means of siRNA) might inhibit the retinal neuronal death induced by either ER stress (tunicamycin) or *N*-methyl-D-aspartate (NMDA).

Materials and Methods

All experiments were performed in accordance with the ARVO Statement for the Use of Animals in Ophthalmic and Vision Research and were approved and monitored by the Institutional Animal Care and Use Committee of Gifu Pharmaceutical University.

Dulbecco modified Eagle medium (DMEM) was purchased from Sigma-Aldrich (St. Louis, MO). The drugs used and their sources were as follows: double-stranded RNA-dependent protein kinase (PKR) inhibitor {8-[imidazol-4-ylmethylene]-6H-azolidino[5,4-g]benzothiazol-7-1}[11] and tunicamycin were obtained from Calbiochem (San Diego, CA) and Wako (Osaka, Japan), respectively; isoflurane was acquired from Nissan Kagaku (Tokyo, Japan); and fetal bovine serum (FBS) was obtained from Valeant (Costa Mesa, CA).

Retinal Ganglion Cell Line Culture

Cultures of RGC-5 were maintained in DMEM supplemented with 10% FBS, 100 U/mL penicillin (Meiji Seika Kaisha, Ltd., Tokyo, Japan), and 100 μg/mL streptomycin (Meiji Seika Kaisha, Ltd.) in a humidified atmosphere of 95% air and 5% CO_2 at 37°C. RGC-5 cells were passaged by trypsinization every 3 days, as described in a previous report.[12]

Cell Viability Assay after Tunicamycin

RGC-5 cells were plated at a density of 1000 cells/well in 96-well culture plates (Falcon 3072; Becton Dickinson Labware, Oxnard, CA). Twenty-four hours later, cells were washed twice with DMEM and then immersed in DMEM supplemented with 1% FBS. One hour later, tunicamycin at 1 to 4 μg/mL was added to the media. Vehicle or PKR inhibitor at 0.03 to 1 μM was added to the media 1 hour before, concomitantly with, or 6 hours after tunicamycin treatment. Twenty-four hours after the addition of tunicamycin, cell viability was measured according to one of two methods. The first was a single-cell digital imaging-based method using fluorescent staining of nuclei. Briefly, cell death was assessed on the basis of combination staining with fluorescent dyes, namely, Hoechst 33342 (Molecular Probes, Eugene, OR) and YO-PRO-1 (YO; Molecular Probes) or propidium iodide (PI; Molecular Probes), observations made using an inverted epifluorescence microscope (IX70; Olympus, Tokyo, Japan). At the end of the culture period, Hoechst 33342 and YO-PRO-1 or PI dyes were added to the culture medium (8 μM, 0.1 μM, and 1.5 μM, respectively) for 30 minutes. Images were collected with a digital camera (Coolpix 4500; Nikon, Tokyo, Japan). At least 400 cells per condition were counted by a masked observer who used image-processing software (ImageJ, version 1.33f; National Institutes of Health, Bethesda, MD). Cell mortality was quantified by expressing the number of YO-PRO-1- or PI-positive cells as a percentage of the number of Hoechst 33342-positive cells.

As the second method for measuring cell viability, the effect on cell viability of tunicamycin treatment was quantitatively assessed by examining the fluorescence intensity changes induced by the cellular reduction of resazurin to resorufin. These experiments were performed in DMEM at 37°C. Cell viability was assessed by the use of 10% resazurin solution for 3 hours at 37°C, and then cells were examined for fluorescence at 560/590 nm. Fluorescence was expressed as a percentage of that in control cells in DMEM containing 1% FBS (after subtraction of background fluorescence).

RNA Interference

For rat PKR and negative control siRNAs, we used a duplex (Stealth PKR RNAi; Invitrogen, Carlsbad, CA) and a control duplex (Stealth RNAi Negative Control Duplex; no. 12935 to 200; Low GC Duplex; Invitrogen), respectively. Sense and antisense strands of rat PKR siRNA were: sequence 1, 5′-UACUUUGUGUAUCUGGGAGUAUUUG-3′ (sense) and 5′-CAAAUACUCCCAGAUACACAAAGUA-3′ (antisense); sequence 2, 5′-AAUUCCAUUUGGAUAAAGAGGCACC-3′ (sense) and 5′-GGUGCCUCUUUAUCCAAAUGGAAUU-3′ (antisense).

Transfection with siRNA In Vitro

RGC-5 cells were seeded at a density of 1000 cells/well into 96-well plates (for cell viability assay) or at a density of 5000 cells/well into 24-well plates (for assessment of the effects of PKR silencing) using the standard medium. Twenty-four hours later, cells were washed twice with medium (Opti-Mem I; Invitrogen) supplemented with 1% FBS without antibiotics and then were immersed in the same medium. Reagent (Lipofectamine 2000; Invitrogen) was used as the transfection agent. PKR and control siRNAs, each at a concentration of 10 nM, were transfected by incubation for 6 hours, according to the manufacturer's instructions (Invitrogen). Subsequently, the medium containing siRNA and complex (Lipofectamine 2000; Invitrogen) was replaced by DMEM supplemented with 1% FBS. Forty-eight hours after the infection, tunicamycin was added to each well, and incubation continued for another 24 hours.

In Vivo NMDA–Induced Retinal Damage

Male adult ddY mice weighing 36 to 43 g each (Japan SLC, Hamamatsu, Japan) were used for these experiments and were kept under controlled lighting conditions (12 hours light/12 hours dark). Anesthesia was induced with 3.0% isoflurane and maintained with1.5% isoflurane in 70% N_2O and 30% O_2, delivered through an animal general anesthesia machine (Soft Lander; Sin-ei Industry Co. Ltd., Saitama, Japan). Body temperatures were maintained between 37.0°C and 37.5°C with the aid of a heating pad and a heating lamp. Retinal damage was induced by injection (2 μL/eye) of NMDA (Sigma-Aldrich) at 10 mM dissolved in 0.01 M phosphate-buffered saline (PBS) injected into the vitreous body of the left eye under the anesthesia described. One drop of levofloxacin ophthalmic solution (Santen Pharmaceuticals Co. Ltd., Osaka, Japan) was applied topically to the treated eye after the intravitreous injection. The PKR inhibitor (1 nmol/eye) or an identical volume of vehicle (0.5% DMSO in PBS) was coadministered with NMDA injection at 20 nmol/eye.

Immunoblotting

RGC-5 cells were lysed using a cell-lysis buffer (RIPA buffer [R0278; Sigma] with protease [P8340; Sigma] and phosphatase inhibitor cocktails [P2850 and P5726; Sigma]; and 1 mM EDTA). Cell lysates were solubilized in SDS-sample buffer, separated on 10% SDS-polyacrylamide gels, and transferred to PVDF membrane (Immobilon-P; Millipore, Bedford, MA). Transfers were blocked for 1 hour at room temperature (5% Blocking One-P; Nakarai Tesque, Inc., Kyoto, Japan) in 10 mM Tris-buffered saline with 0.05% Tween 20 (TBS-T) and were incubated overnight at 4°C with the primary antibody. Transfers were then rinsed with TBS-T and incubated for 1 hour at room temperature in horseradish peroxidase goat anti-rabbit or goat anti-mouse (Pierce, Rockford, IL) diluted 1:2000. Immunoblots were developed with chemiluminescence (Super Signal West Femto Maximum Sensitivity Substrate; Pierce) and visualized with the aid of a digital imaging system (FAS-1000; Toyobo Co., Ltd., Osaka, Japan). Primary antibodies used were as follows: mouse anti-BiP (BD Bioscience, San Jose, CA), rabbit anti-ATF4 (Santa Cruz Biotechnology, Santa Cruz, CA), rabbit anti-phospho-PKR (Abcam, Cambridge, MA), rabbit anti-PKR (Cell Signaling, Beverly, MA), mouse anti-CHOP (Santa Cruz Biotechnology), and rabbit anti-actin (Santa Cruz Biotechnology).

Immunostaining

To clarify whether NMDA or tunicamycin induced PKR phosphorylation in the mouse retina in vivo and whether a PKR inhibitor would prevent PKR phosphorylation, immunocytochemistry was performed. At 12 or 24 hours after intravitreal injection of NMDA (20 mmol/eye) or tunicamycin (1 μg/eye), with or without PKR inhibitor (1 nmol/eye), eyes were enucleated, fixed in 4% paraformaldehyde overnight at 4°C, immersed in 20% sucrose for 48 hours at 4°C, and embedded in optimum cutting temperature (OCT) compound (Sakura Finetechnical Co., Ltd., Tokyo, Japan). Transverse, 10-μm–thick cryostat sections were cut and placed onto slides (Mas Coat). Sections were subsequently processed for immunocytochemistry using antibodies against phospho-PKR (Abcam) diluted 1:500 in immunoreaction enhancer solution A (CanGet signal immunostain; Toyobo Co., Ltd.). Sections were incubated with biotin-conjugated secondary antibody for 1 hour at room temperature and were visualized with an immunodetection kit (Vector M.O.M.; Vector, Burlingame, CA).

Histologic Analysis of Mouse Retina

Seven days after the NMDA or tunicamycin injection, eyeballs were enucleated for histologic analysis. In mice under anesthesia produced by intraperitoneal injection of sodium pentobarbital (80 mg/kg), each eye was enucleated and kept immersed for at least 24 hours at 4°C in a fixative solution containing 4% paraformaldehyde. Six paraffin-embedded sections (3-μm thick) cut through the optic disc of each eye were prepared in a standard manner and were stained with hematoxylin and eosin. Retinal damage was evaluated as described previously, with three sections from each eye used for the morphometric analysis. Light microscope images were photographed, and the cell counts in the ganglion cell layer (GCL), at a distance between 350 and 650 μm from the optic disc, were measured on the photographs in a masked fashion by a single observer (Y.I.). Data from three sections (selected

randomly from the six sections) were averaged for each eye, and the values obtained were used to evaluate the cell count in the GCL.

Statistical Analysis

Data are presented as the mean ± SEM. Statistical comparisons were made, using a Student's *t*-test or a Dunnett test (by means of Stat View version 5.0; SAS Institute Inc., Cary, NC). $P < 0.05$ was considered statistically significant.

Results

Retinal Cell Death and Changes in Endoplasmic Reticulum Stress-Related Protein Induced by Tunicamycin

The time-course of the changes in cell morphology occurring after tunicamycin treatment at 2 μg/mL are shown in Figure 1A. An increase in nonadherent cells was observed 12 hours after tunicamycin treatment compared with that in nontreated control cells. Representative fluorescence stainings of nuclei—using Hoechst 33342, YO-PRO-1, and propidium iodide (PI) dyes—are shown in Figure 1B. Nontreated control cells displayed normal nuclear morphology and negative staining with YO-PRO-1 dye (which stains early apoptotic and later-stage cells) and PI dye (which stains late-stage apoptotic cells) (Fig. 1B, upper panels). Treatment with tunicamycin led to shrinkage and condensation of nuclei and to positive staining with each of these dyes (Fig. 1B, lower panels).

Changes in the protein levels of BiP, pATF-4, and CHOP 24 hours after tunicamycin treatment at 1–4 μg/mL are shown in Figure 1C. BiP, ATF-4, and CHOP were all concentration dependently increased, whereas actin levels remained unchanged.

Phosphorylation of a PKR in RGC-5 Cells Is Induced by Tunicamycin

Although no phosphorylated PKR was observed in vehicle-treated normal cells, marked and slight increases in phosphorylated PKR were noted at 6 and 24 hours, respectively, after tunicamycin treatment (Fig. 2A).

Effects of a PKR Inhibitor and PKR Silencing on the RGC-5 Cell Death Induced by Tunicamycin

Representative fluorescence stainings of nuclei with Hoechst 33342 and YO-PRO-1 dyes are shown in Figure 2B. Nontreated cells showed normal nuclear morphology and negative staining with YO-PRO-1 dye (which stains early-stage apoptotic and necrotic cells). Treatment with tunicamycin at 2 μg/mL for 24 hours led to shrinkage and condensation of nuclei and to positive staining with YO-PRO-1 dye. Treatment with a PKR inhibitor at 0.3 and 1 μM reduced the tunicamycin-induced morphologic changes in nuclei and the number of cells stained with YO-PRO-1. The number of cells exhibiting YO-PRO-1 fluorescence was counted, and the positive cells were expressed as the percentage of YO-PRO-1– to Hoechst 33342–

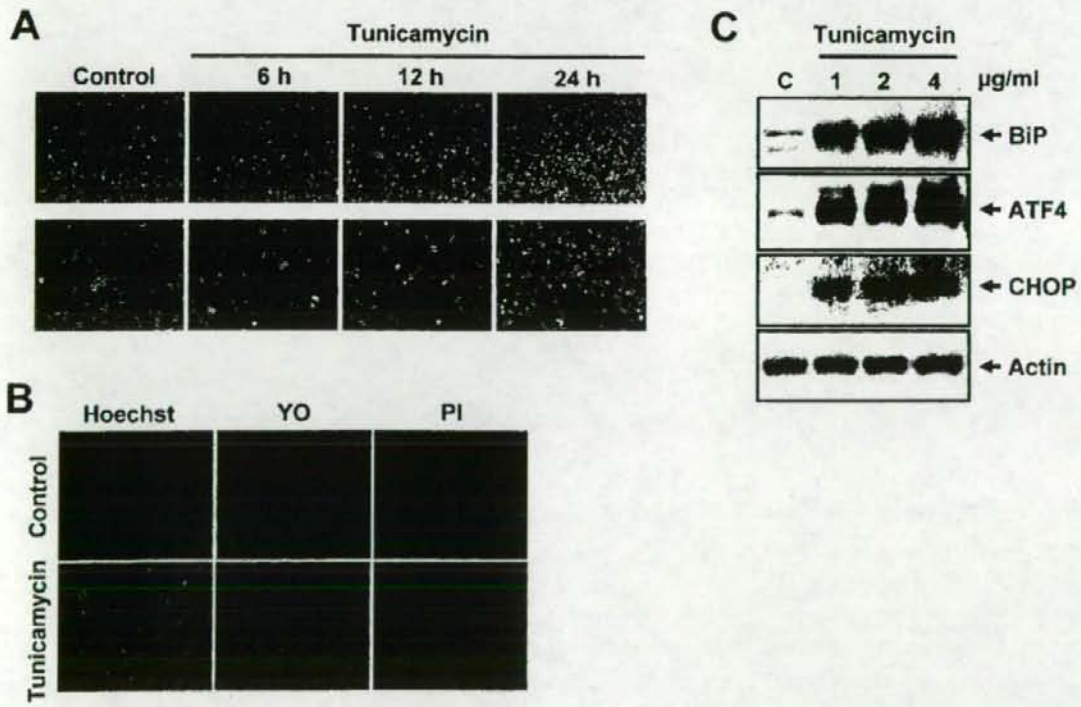

FIGURE 1. RGC-5 cell death and changes in ER-stress related proteins induced by tunicamycin. (A) Representative phase-contrast microscopy showing time-course of changes in RGC-5 cells after addition of tunicamycin at 2 μg/mL (*upper panels*, low power; *lower panels*, high power). Bar = 250 μm. (B) Representative fluorescence microscopy showing nuclear stainings for Hoechst 33342, YO-PRO-1, and PI 24 hours after tunicamycin treatment at 2 μg/mL. (C) Representative immunoblots showing protein levels (BiP, ATF4, CHOP, and actin) 24 hours after tunicamycin treatment at 1–4 μg/mL.

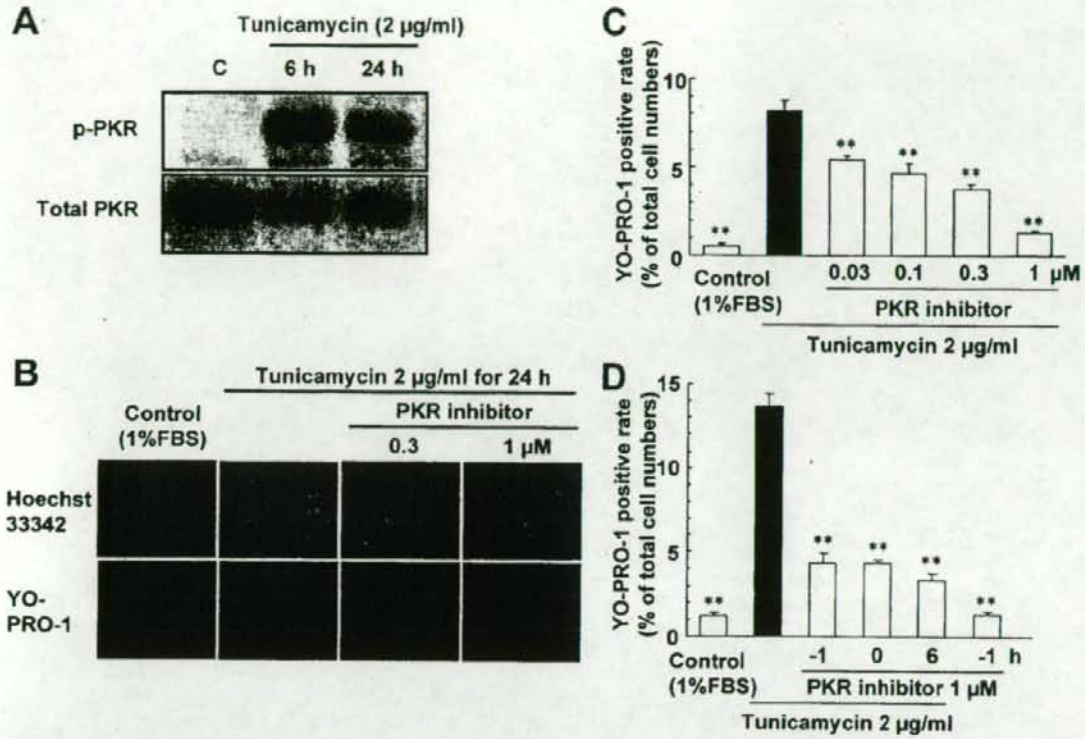

FIGURE 2. Phosphorylation of a PKR and its inhibitory effect on tunicamycin-induced cell damage in RGC-5 cells. (A) Phosphorylation of PKR in RGC-5 cells is induced by tunicamycin. Representative band images show immunoreactivity toward phosphorylated PKR and total PKR. (B–D) Effects of a PKR inhibitor on the RGC-5 cell death induced by tunicamycin. (B) Representative fluorescence microscopy showing nuclear stainings for Hoechst 33342 and YO-PRO-1 after 24-hour tunicamycin treatment. The PKR inhibitor was added 1 hour before the tunicamycin. (C) Number of cells exhibiting YO-PRO-1 fluorescence was counted, and positive cells were expressed as the percentage of YO-PRO-1 to Hoechst 33342. Each column represents the mean ± SEM ($n = 8$). $^{**}P < 0.01$ versus tunicamycin alone (Dunnett test). (D) The PKR inhibitor at 1 μM was added 1 hour before, concomitantly with, or 6 hours after tunicamycin at 2 μg/mL. Number of cells exhibiting YO-PRO-1 fluorescence was counted, and the positive cells were expressed as the percentage of YO-PRO-1 to Hoechst 33342. Each column represents the mean ± SEM ($n = 8$). $^{**}P < 0.01$ versus tunicamycin alone (Dunnett test).

positive cells (Fig. 2C). After treatment with tunicamycin for 24 hours, the percentage of YO-PRO-1-positive cells was 8.2% ± 0.5% ($n = 8$), whereas in the control group (supplemented with 1% FBS) it was 0.5% ± 0.1% ($n = 8$). Treatment with the PKR inhibitor at 0.03 to 1 μM significantly reduced the increase in YO-PRO-1-positive cells induced by tunicamycin (in a concentration-dependent manner). Treatment with the PKR inhibitor at 1 μM, either concomitantly with or 6 hours after tunicamycin, protected against RGC-5 cell death at 24 hours after tunicamycin (Fig. 2D). As shown in Figures 3A and 3B, each of the PKR siRNAs (#1 and #2) that recognize nonoverlapping sequences of rat PKR decreased the PKR protein ex-

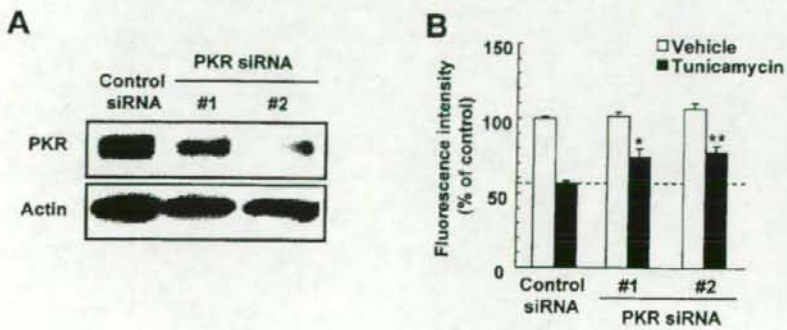

FIGURE 3. Effect of PKR siRNAs on tunicamycin-induced RGC-5 cell death. (A) Representative band images show immunoreactivities toward PKR and actin. PKR protein was decreased by 48-hour treatment with one of two PKR siRNAs. (B) RGC-5 cells were transiently transfected with control siRNA or one of two PKR siRNAs. After 48 hours, cells were treated with 2 μg/mL tunicamycin and maintained in this condition for another 24 hours. Each column represents the mean ± SEM ($n = 8$). $^{*}P < 0.05$ and $^{**}P < 0.01$ versus control siRNA-treated group (Dunnett test).

pression and led to a significant level of resistance to the tunicamycin-induced decrease in cell viability. Some standard siRNAs have been reported to induce the activation of PKR/interferon pathways as nonspecific stress responses resulting in growth inhibition and cytotoxicity.[13] To avoid such undesirable responses, we used duplex and control duplex siRNA (Stealth; Invitrogen) with chemical modifications to enable the elimination of nonspecific stress response affecting the PKR/interferon pathways.[14] In the present study, negative control siRNA (Stealth; Invitrogen) at 10 nM did not increase PKR protein at 48 hours after treatment compared with the nontreated control (Shimazawa et al., unpublished data, 2006). This result indicates that under our experimental conditions, Stealth siRNA does not induce the activation of PKR/interferon pathways.

Effects of a PKR Inhibitor on the Tunicamycin-Induced Increases in BiP and CHOP Proteins in RGC-5 Cells

To determine the mechanism underlying the action of tunicamycin, we examined the effect of the PKR inhibitor on the increases in BiP and CHOP proteins induced in RGC-5 cells by treatment with tunicamycin at 2 μg/mL for 24 hours. Tunicamycin induced BiP and CHOP proteins in such cells (Fig. 4). Pretreatment with the PKR inhibitor at 1 μM significantly reduced the increase in CHOP protein but not that in BiP protein. On the other hand, treatment with the same PKR inhibitor alone (at 0.3 or 1 μM) had little effect on the production of these proteins (vs. vehicle-treated controls). Staurosporine (200 nM), an apoptosis inducer, did not increase BiP or CHOP protein, but it did induce apoptotic cell death in this condition.

Phosphorylation of a PKR in Mouse Retina after NMDA or Tunicamycin

No phosphorylated PKR was observed in the vehicle-treated normal retina, but phosphorylated PKR was observed in both the GCL and the inner plexiform layer (IPL) at 12 and 24 hours after intravitreal injection of NMDA (Fig. 5). Phosphorylated PKR was also observed in GCL and IPL at 12 and 24 hours after tunicamycin injection (Fig. 5). The PKR inhibitor (1 nmol), when coadministered with NMDA or tunicamycin, inhibited the increases in phosphorylated PKR in mouse retina induced by NMDA and tunicamycin (Fig. 5).

Effect of a PKR Inhibitor on the Retinal Damage Induced by Intravitreal Injection of NMDA

Intravitreal injection of NMDA at 20 nmol/eye decreased the cell count in the GCL (vs. nontreated normal retinas; Figs. 6A, 6B). Coadministration of the PKR inhibitor at 1 nmol/eye significantly reduced the NMDA-induced loss of GCL cells (Figs. 6A, 6B).

Discussion

In the present study, we demonstrated a close association between PKR and ER stress-induced retinal damage and showed that the inhibition of PKR reduced such damage.

Nutrient deprivation and agents that cause unfolded or misfolded proteins in the ER can activate the ER stress response, though the cell normally survives the insult.[1] However, excessive or prolonged ER stress can induce cell death, usually in the form of apoptosis. In the present study, we found that tunicamycin induced the ER stress-associated proteins BiP, ATF-4, and CHOP in cultured RGC-5 cells. In our previous study, the phosphorylation of eukaryotic translation initiation factor 2 kinase (eIF2α) was increased concomitantly with the increases in the expressions of BiP, ATF-4, and CHOP proteins from 6 hours onward.[15] BiP, ATF-4, and the phosphorylation of eIF2α increased time-dependently throughout the 24-hour tunicamycin treatment period, whereas actin levels remained unchanged. CHOP was first detected 6 hours after the addition of tunicamycin, and it persisted thereafter. On the other hand, a slight increase in cell death was observed 12 hours after tunicamycin treatment, and it was time-dependently increased thereafter.[15] BiP acts as an ER-resident molecular chaperone induced by ER stress, and this protein refolds the unfolded proteins, thereby tending to maintain homeostasis in the ER.[16,17] CHOP is a member of the CCAAT/enhancer-binding protein family that is induced by ER stress and participates in ER-mediated apoptosis; hence, CHOP may be a key molecule in retinal cell death.[18]

PKR is involved in the phosphorylation of eIF2α.[19,20] Overexpression of PKR leads to apoptosis.[21] In recent years, PKR

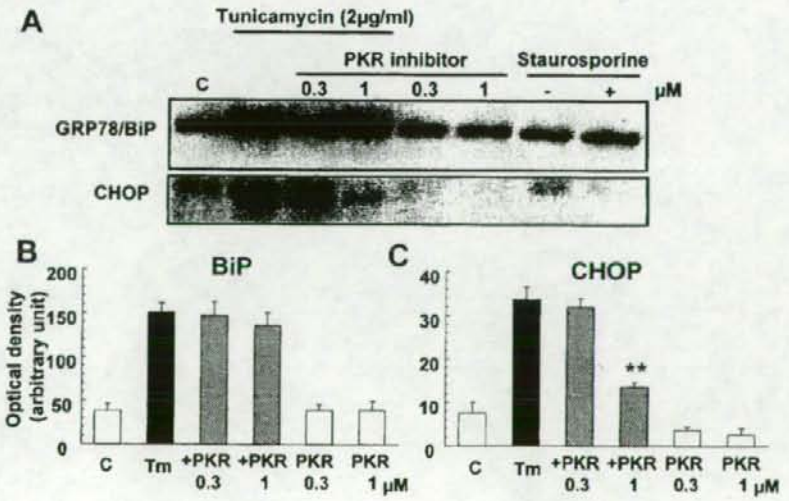

FIGURE 4. Effect of a PKR inhibitor on the tunicamycin-induced increases in BiP and CHOP proteins in RGC-5 cells. (A) Representative band images show immunoreactivities against BiP and CHOP. Quantitative analysis of band densities for BiP (B) and CHOP (C). Data are expressed as mean ± SEM ($n = 4$) of values (in arbitrary units) obtained from each band. $^{**}P < 0.01$ versus tunicamycin alone (Dunnett test).

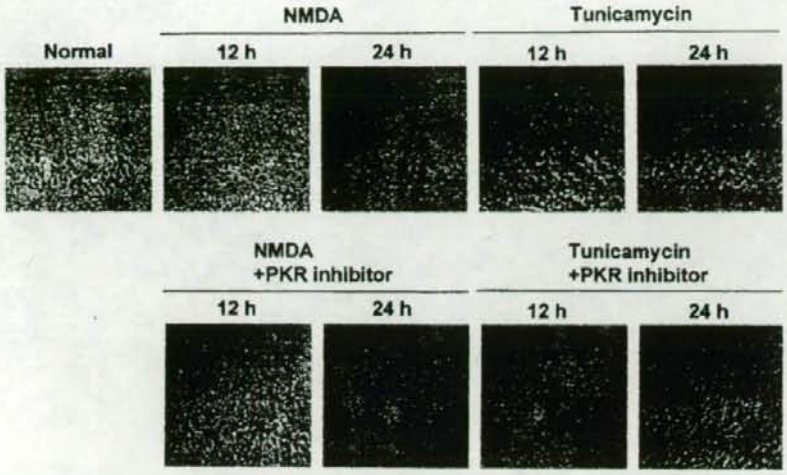

FIGURE 5. Phosphorylation of a PKR in mouse retina is induced by NMDA and by tunicamycin. Retinal cross-sections were labeled with antibody against phosphorylated PKR. Phospho-PKR-like immunoreactivity was increased in the inner retina 12 and 24 hours after intravitreal injection of NMDA (20 nmol/eye) or of tunicamycin (1 μg/eye). Coadministration of PKR inhibitor (1 nmol/eye) with the NMDA or tunicamycin inhibited the increase in phosphorylated PKR. Bar = 25 μm.

has been reported to be involved in Alzheimer disease,[7,22–24] Huntington disease,[25] Parkinson disease,[26] and amyotrophic lateral sclerosis,[27] indicating that PKR may be implicated in the neuronal damage induced by ER stress in these neurologic diseases. In the present study, PKR phosphorylation was observed in RGC-5 cells 6 and 24 hours after tunicamycin treatment. We therefore tested, both in vitro and in vivo, whether the activation of PKR might participate in the retinal neuron death induced by ER stress. In the in vitro study, both the PKR inhibitor and the knockdown of PKR (using siRNA) inhibited tunicamycin-induced RGC-5 cell death, and the inhibitor attenuated the tunicamycin-induced increase in CHOP protein but not the tunicamycin-induced BiP protein production. In our previous study, we reported that the same PKR inhibitor protects against the cell death induced by tunicamycin in a different cell line, SH-SY5Y cells.[28] Furthermore, treatment with the PKR inhibitor at 1 μM, either concomitantly with or 6 hours after tunicamycin, protected against RGC-5 cell death 24 hours after tunicamycin. This result suggests that PKR may operate in the late phase. In this study, *pretreatment* with the PKR inhibitor at 1 μM reduced the expression of CHOP protein 24 hours after tunicamycin. However, treatment with the PKR inhibitor (1 μM) *6 hours after* tunicamycin, when CHOP protein was being induced, also protected against RGC-5 cell death. This result suggests that CHOP production does not necessarily have to be decreased for cell survival to be enhanced. Indeed, pretreatment with the PKR inhibitor at 0.3 μM also inhibited tunicamycin-induced RGC-5 cell death, but it did not reduce the increase in CHOP protein. Although CHOP-deficient mice have been reported to show resistance to ER stress-induced cell death, a dimerization partner such as C/EBPβ is needed for the induction of such cell death.[29] In addition, CHOP protein

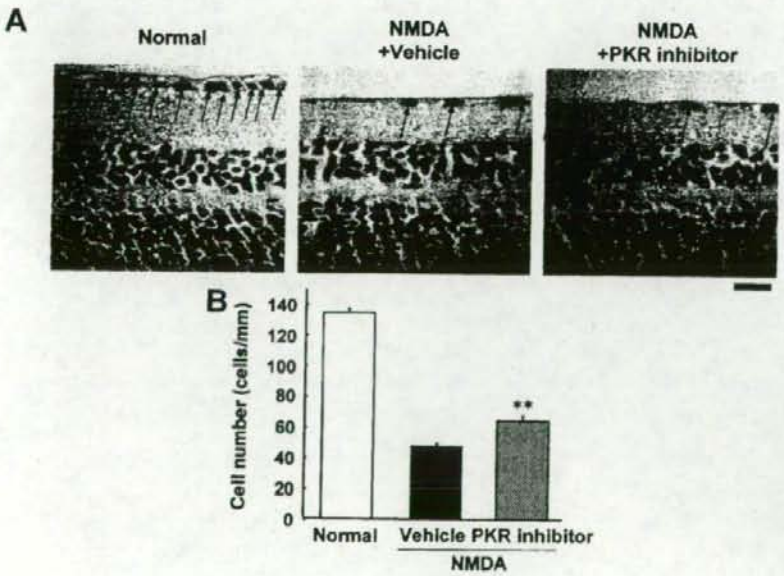

FIGURE 6. Effect of a PKR inhibitor on the mouse retinal damage induced by intravitreal injection of NMDA. (A) Representative photographs showing nontreated normal retina, NMDA-injected vehicle-treated retina, and NMDA-injected PKR inhibitor-treated retina. PKR inhibitor at 1 nmol/eye or vehicle was coadministered with the NMDA (20 nmol/eye). Quantitative analysis of cell number in the GCL (B). Each column represents the mean ± SEM ($n = 12$). $^{**}P < 0.01$ versus NMDA plus vehicle-treated group (Student's *t*-test). Bar = 25 μm.

undergoes stress-inducible phosphorylation by stress-inducible members of the p38 mitogen-activated protein kinase (MAPK) family, and such phosphorylation is associated with an enhancement of transcriptional activation by CHOP.[30] Takizawa et al.[31] reported that a dominant-negative mutant of PKR inhibited the apoptosis and the p38 MAPK activation induced by apoptosis signal-regulating kinase 1 (ASK1), a member of the MAPK kinase kinase (MAPKKK) family, which is activated by a variety of apoptosis-inducers. Both ASK1 and PKR are known to bind proteins associated with death receptors, such as tumor necrosis factor (TNF) receptor–associated protein 2 (TRAF2).[32,33] During ER-stress, ASK1 is recruited to oligomerized inositol-requiring enzyme-1 (IRE1) complexes containing TRAF2, thereby activating this kinase and causing downstream activation of c-Jun N-terminal kinase (JNK) and p38 MAPK.[34] Thus, PKR may activate the ASK1-p38 MAPK/-JNK signaling pathways to execute apoptosis. Furthermore, aggregated β-amyloid peptide has been reported to activate PKR through its phosphorylation or cleavage through calcium release from the ER, with activation of caspase-8 and caspase-3 as upstream signals.[23] In another possible mechanism, the eIF2α phosphorylation induced by activated PKR might result in an upregulation of CHOP, a proapoptotic transcription factor. In addition, excessive ER stress leads to activation of PKR-like ER kinase (PERK), just as it does to activation of PKR.[35,36] The luminal ER stress-sensing domains of PERK regulate its dimerization, and this leads to activation of its protein kinase activity under ER stress. Activation of PERK induces phosphorylation of eIF2α, contributing to a suppression of protein translation after the initiation of ER stress. Therefore, even when PKR activation is inhibited by a PKR inhibitor or by PKR downregulation (using siRNA), the phosphorylation of eIF2α may not be reduced. Accordingly, eIF2α may not be a target molecule through which activated PKR executes cell death, at least in ER stress. However, further studies will be needed to clarify the precise mechanisms. Regarding the specificity of the PKR inhibitor against PKR, we must consider the possibility of effects on other targets as a limitation.

The present results were obtained in cultured RGC-5 cells, and it could be agreed that the protective effect observed in vitro cannot be extrapolated directly to animal models in vivo. However, we have already confirmed that intravitreal injection of NMDA leads to increases in X box binding protein (XBP-1) mRNA splicing and in BiP and CHOP proteins in the mouse retina, representing activation of the unfolded protein response (UPR) signaling pathway.[15] Moreover, expression of the CHOP gene is reportedly increased in the rat retina after intravitreal injection of NMDA.[37] Furthermore, Awai et al.[38] found that treatment with MK-801, an NMDA-receptor antagonist, inhibited the increases in CHOP mRNA and protein in the mouse retina observed after intravitreal injection of NMDA and that CHOP-deficient mice were resistant to NMDA-induced retinal damage. However, CHOP-deficient mice partially suppressed NMDA-induced retinal cell death; therefore, other pathways (e.g., leading to mitochondrial dysfunction) may be engaged in the induction of this cell death. These findings indicate that NMDA can cause ER stress in the retina and that the neurotoxicity induced by NMDA is caused in part by a mechanism dependent on the induction of CHOP protein through excessive ER stress. On the other hand, the neuroprotective effect of the PKR inhibitor on tunicamycin-induced RGC-5 cell death did not appear to depend on CHOP suppression. Although little is known about the precise mechanisms responsible for the NMDA-induced activation of ER stress, NMDA is known to cause intracellular Ca^{2+} overload and increased NO production, resulting in apoptotic cell death.[39,40] Several lines of study suggest that intracellular Ca^{2+} overload and excessive production of NO deplete Ca^{2+} in the ER, thereby resulting in ER stress.[41,42] Recently, Uehara et al.[43] reported that in primary cortical culture, even mild exposure to NMDA induces apoptotic cell death through an accumulation of polyubiquitinated proteins and increases in XBP-1 mRNA splicing and CHOP mRNA, representing activation of the UPR signaling pathway. Furthermore, they found that NO induces S-nitrosylation of protein-disulfide isomerase (PDI), an enzyme that assists in the maturation and transport of unfolded secretory proteins and thereby helps to prevent the neurotoxicity associated with ER stress. S-nitrosylated PDI exhibits reduced enzymatic activity and induces cell death through the ER stress pathway. These mechanisms may contribute to the activation of ER stress in the retina after NMDA stimulation. Collectively, the results indicate that NMDA can cause ER stress in the retina and that the neurotoxicity induced by NMDA is caused in part by a mechanism dependent on ER stress.

In the present study, the phosphorylation of PKR was increased in the inner retina in mice in vivo after intravitreal injection of either NMDA or tunicamycin. The PKR inhibitor, when coadministered with NMDA or tunicamycin, inhibited the increase in phosphorylated PKR. This result indicates that PKR may be activated in the mouse retina in vivo during ER stress. The PKR inhibitor also reduced NMDA-induced retinal damage in mice in vivo, but this was a partial effect. Possibly, the observed difference in potency between the in vitro and in vivo situations may be attributed to the poor distribution or rapid excretion in ocular tissues of the PKR inhibitor after its intravitreal injection. Taken together, our results indicate that ER stress plays a role in retinal ganglion cell death and that PKR activation forms part of the underlying mechanisms.

In conclusion, we have identified a close association between PKR and ER stress–induced retinal damage, and our results suggest that PKR might be a good target in the search for better treatments for retinal diseases.

Acknowledgments

The authors thank Neeraj Agarwal (Department of Pathology and Anatomy, UNT Health Science Center, Forth Worth, TX) for the kind gift of RGC-5.

References

1. Kaufman RJ. Stress signaling from the lumen of the endoplasmic reticulum: coordination of gene transcriptional and translational controls. *Genes Dev*. 1999;13:1211–1233.
2. Harding HP, Calfon M, Urano F, Novoa I, Ron D. Transcriptional and translational control in the mammalian unfolded protein response. *Annu Rev Cell Dev Biol*. 2002;18:575–599.
3. Aridor M, Balch WE. Integration of endoplasmic reticulum signaling in health and disease. *Nat Med*. 1999;5:745–751.
4. Bonne C, Muller A, Villain M. Free radicals in retinal ischemia. *Gen Pharmacol*. 1998;30:275–280.
5. Dreyer EB. A proposed role for excitotoxicity in glaucoma. *J Glaucoma*. 1998;7:62–67.
6. Neufeld AH. Nitric oxide: a potential mediator of retinal ganglion cell damage in glaucoma. *Surv Ophthalmol*. 1999;43(suppl 1):S129–S135.
7. Onuki R, Bando Y, Suyama E, et al. An RNA-dependent protein kinase is involved in tunicamycin-induced apoptosis and Alzheimer's disease. *EMBO J*. 2004;23:959–968.
8. Gale M Jr, Katze MG. Molecular mechanisms of interferon resistance mediated by viral-directed inhibition of PKR, the interferon-induced protein kinase. *Pharmacol Ther*. 1998;78:29–46.
9. Wu S, Kaufman RJ. A model for the double-stranded RNA (dsRNA)-dependent dimerization and activation of the dsRNA-activated protein kinase PKR. *J Biol Chem*. 1997;272:1291–1296.
10. Srivastava SP, Kumar KU, Kaufman RJ. Phosphorylation of eukaryotic translation initiation factor 2 mediates apoptosis in response

to activation of the double-stranded RNA-dependent protein kinase. *J Biol Chem*. 1998;273:2416–2423.
11. Jammi NV, Whitby LR, Beal PA. Small molecule inhibitors of the RNA-dependent protein kinase. *Biochem Biophys Res Commun*. 2003;308:50–57.
12. Krishnamoorthy RR, Agarwal P, Prasanna G, et al. Characterization of a transformed rat retinal ganglion cell line. *Brain Res Mol Brain Res*. 2001;86:1–12.
13. Puthenveetil S, Whitby L, Ren J, Kelnar K, Krebs JF, Beal PA. Controlling activation of the RNA-dependent protein kinase by siRNAs using site-specific chemical modification. *Nucleic Acids Res*. 2006;34:4900–4911.
14. Carstea ED, Hough S, Wiederholt K, Welch PJ. State-of-the-art modified RNAi compounds for therapeutics. *IDrugs*. 2005;8:642–647.
15. Shimazawa M, Inokuchi Y, Ito Y, et al. Involvement of ER stress in retinal cell death. *Mol Vis*. 2007;13:578–587.
16. Kleizen B, Braakman I. Protein folding and quality control in the endoplasmic reticulum. *Curr Opin Cell Biol*. 2004;16:343–349.
17. Gething MJ. Role and regulation of the ER chaperone BiP. *Semin Cell Dev Biol*. 1999;10:465–472.
18. Oyadomari S, Mori M. Roles of CHOP/GADD153 in endoplasmic reticulum stress. *Cell Death Differ*. 2004;11:381–389.
19. Williams BR. PKR: a sentinel kinase for cellular stress. *Oncogene*. 1999;18:6112–6120.
20. Kumar KU, Srivastava SP, Kaufman RJ. Double-stranded RNA-activated protein kinase (PKR) is negatively regulated by 60S ribosomal subunit protein L18. *Mol Cell Biol*. 1999;19:1116–1125.
21. Donze O, Dostie J, Sonenberg N. Regulatable expression of the interferon-induced double-stranded RNA dependent protein kinase PKR induces apoptosis and fas receptor expression. *Virology*. 1999;256:322–329.
22. Peel AL, Bredesen DE. Activation of the cell stress kinase PKR in Alzheimer's disease and human amyloid precursor protein transgenic mice. *Neurobiol Dis*. 2003;14:52–62.
23. Suen KC, Yu MS, So KF, Chang RC, Hugon J. Upstream signaling pathways leading to the activation of double-stranded RNA-dependent serine/threonine protein kinase in beta-amyloid peptide neurotoxicity. *J Biol Chem*. 2003;278:49819–49827.
24. Chang RC, Suen KC, Ma CH, Elyaman W, Ng HK, Hugon J. Involvement of double-stranded RNA-dependent protein kinase and phosphorylation of eukaryotic initiation factor-2alpha in neuronal degeneration. *J Neurochem*. 2002;83:1215–1225.
25. Peel AL, Rao RV, Cottrell BA, Hayden MR, Ellerby LM, Bredesen DE. Double-stranded RNA-dependent protein kinase, PKR, binds preferentially to Huntington's disease (HD) transcripts and is activated in HD tissue. *Hum Mol Genet*. 2001;10:1531–1538.
26. Bando Y, Onuki R, Katayama T, et al. Double-strand RNA dependent protein kinase (PKR) is involved in the extrastriatal degeneration in Parkinson's disease and Huntington's disease. *Neurochem Int*. 2005;46:11–18.
27. Hu JH, Zhang H, Wagey R, Krieger C, Pelech SL. Protein kinase and protein phosphatase expression in amyotrophic lateral sclerosis spinal cord. *J Neurochem*. 2003;85:432–442.
28. Shimazawa M, Hara H. Inhibitor of double stranded RNA-dependent protein kinase protects against cell damage induced by ER stress. *Neurosci Lett*. 2006;409:192–195.
29. Zinszner H, Kuroda M, Wang X, et al. CHOP is implicated in programmed cell death in response to impaired function of the endoplasmic reticulum. *Genes Dev*. 1998;12:982–995.
30. Wang XZ, Ron D. Stress-induced phosphorylation and activation of the transcription factor CHOP (GADD153) by p38 MAP kinase. *Science*. 1996;272:1347–1349.
31. Takizawa T, Tatematsu C, Nakanishi Y. Double-stranded RNA-activated protein kinase interacts with apoptosis signal-regulating kinase, 1: implications for apoptosis signaling pathways. *Eur J Biochem*. 2002;269:6126–6132.
32. Gil J, Garcia MA, Gomez-Puertas P, et al. TRAF family proteins link PKR with NF-kappa B activation. *Mol Cell Biol*. 2004;24:4502–4512.
33. Nishitoh H, Saitoh M, Mochida Y, et al. ASK1 is essential for JNK/SAPK activation by TRAF2. *Mol Cell*. 1998;2:389–395.
34. Nishitoh H, Matsuzawa A, Tobiume K, et al. ASK1 is essential for endoplasmic reticulum stress-induced neuronal cell death triggered by expanded polyglutamine repeats. *Genes Dev*. 2002;16:1345–1355.
35. Harding HP, Zhang Y, Ron D. Protein translation and folding are coupled by an endoplasmic-reticulum-resident kinase. *Nature*. 1999;397:271–274.
36. Ma K, Vattem KM, Wek RC. Dimerization and release of molecular chaperone inhibition facilitate activation of eukaryotic initiation factor-2 kinase in response to endoplasmic reticulum stress. *J Biol Chem*. 2002;277:18728–18735.
37. Laabich A, Li G, Cooper NG. Characterization of apoptosis-genes associated with NMDA mediated cell death in the adult rat retina. *Brain Res Mol Brain Res*. 2001;91:34–42.
38. Awai M, Koga T, Inomata Y, et al. NMDA-induced retinal injury is mediated by an endoplasmic reticulum stress-related protein, CHOP/GADD153. *J Neurochem*. 2006;96:43–52.
39. Leist M, Volbracht C, Kuhnle S, Fava E, Ferrando-May E, Nicotera P. Caspase-mediated apoptosis in neuronal excitotoxicity triggered by nitric oxide. *Mol Med*. 1997;3:750–764.
40. Bonfoco E, Leist M, Zhivotovsky B, Orrenius S, Lipton SA, Nicotera P. Cytoskeletal breakdown and apoptosis elicited by NO donors in cerebellar granule cells require NMDA receptor activation. *J Neurochem*. 1996;67:2484–2493.
41. Li WW, Alexandre S, Cao X, Lee AS. Transactivation of the grp78 promoter by $Ca2^+$ depletion: a comparative analysis with A23187 and the endoplasmic reticulum Ca(2+)-ATPase inhibitor thapsigargin. *J Biol Chem*. 1993;268:12003–12009.
42. Oyadomari S, Araki E, Mori M. Endoplasmic reticulum stress-mediated apoptosis in pancreatic beta-cells. *Apoptosis*. 2002;7:335–345.
43. Uehara T, Nakamura T, Yao D, et al. S-nitrosylated protein-disulphide isomerase links protein misfolding to neurodegeneration. *Nature*. 2006;441:513–517.

日本神経精神薬理学雑誌（Jpn. J. Neuropsychopharmacol.）27：63-67（2007）

〔特集：学会シンポジウム〕

分子シャペロン誘導剤の神経変性疾患治療への応用*

工藤　喬*1　今泉和則*2　原　英彰*3

*1 大阪大学大学院医学系研究科精神医学教室
*2 宮崎大学医学部解剖学講座
*3 岐阜薬科大学生体機能分子学教室

要約：小胞体（ER）ストレスは，折りたたみ不整な蛋白が細胞内に蓄積することによって生じ，アルツハイマー病などの神経変性疾患の病理過程に関与しているとされる．ERストレスに対し，細胞は反応機構を元来備えており，ストレス状況からの離脱を図る．本研究はERストレス反応機構の1つである分子シャペロン誘導を人為的に行い，ストレスからの離脱を図ることで，アルツハイマー病（AD）などの神経変性疾患の治療に応用しようとするものである．分子シャペロンBiPのプロモーターを用いた解析から，我々はBiP誘導剤（BIX: BiP inducer X）を得た．細胞実験から，BIXはBiPのみ誘導し，他のERストレス反応分子を誘導させないことが示された．また，BIXで処理した細胞はERストレスに耐性を示し，ERのアポトーシス誘導分子の発現を抑えることが示された．さらに，マウスの脳室にBIXを前投与し，脳虚血を負荷すると梗塞巣の面積の減少をもたらし，神経症状の軽減が認められた．このBIXの効果は，梗塞周辺領域でERのアポトーシス誘導分子の発現を抑えることによることが示された．以上のように，BIXはERストレスから生じるアポトーシスを抑制し，ADをはじめとする神経変性疾患の治療薬になることが示唆された．

キーワード：小胞体（ER）ストレス，分子シャペロン，アポトーシス，脳虚血，神経変性疾患

近年，アルツハイマー病（AD）の治療薬開発は，アミロイド前駆体蛋白のβ/γセクレターゼ阻害薬，非ステロイド消炎鎮痛剤，アミロイドワクチンなど様々な可能性が検討されているが，実用化に至ったものは未だない．したがって，現時点では多くの可能性を模索すべき時期であろうと思われる．また，パーキンソン病，レビー小体病，前頭側頭型認知症，ポリグルタミン病などの神経変性疾患は未だ病態過程が不明な点が多く，確立された根治療法がない．ただ，ADを含むこれらの疾患では，異常蛋白が神経細胞内に蓄積凝集するという点が共通であり，興味深い．

我々は，従来からアルツハイマー病の病態を小胞体（ER）ストレスに対する反応，すなわちunfolded protein response（UPR）の見地から検討してきた．このUPRは異常蛋白蓄積に直接リンクしていると考えられ，神経変性疾患研究の1つのトレンドとして多くの検討が行われている．近年我々は，ERストレスについて蓄積してきた知見を踏まえ，治療戦略への応用を検討し始めている．

Unfolded Protein Response（UPR）

細胞小器官の1つであるERは，分泌蛋白や膜構成蛋白などの折りたたみや翻訳後修飾を行う蛋白の「組み立て工場」のような役割を担う．「組み立て工場」であるが故に「不良品」すなわち折りたたみが不十分な，あるいは不正な蛋白（unfolded protein）の出現は宿命のようなものである．様々なストレスは，ERストレスとしてこのunfolded proteinのER内への蓄積を生じ，カスペース12の活性化（Nakagawa et al, 2000）（ヒトではカスペース4（Hitomi et al, 2004））, JNK系路の活性化（Nishitoh et al, 2002），CHOPの誘導（Friedman, 1996）等のER発動のアポトーシスにつながる．その防御機構として，細胞には3つのUPRが備わっている．

1. 分子シャペロンの誘導

UPRの働きの1つは，小胞体から核へのシグナル伝達を活性化し，GRP78/BiPやGRP94などの分子シャペロンを発現誘導することである．これら分子シャペロンは，unfolded proteinに作用し，折りたたみの促進や是正を行う（Sidrauski et al, 1998）．

2. 蛋白翻訳抑制

第2の戦略は，これ以上unfolded proteinを生じないように，蛋白の翻訳自体を抑制する方策であり，翻訳開始因子の$eIF2\alpha$がリン酸化されることで発動される（Harding et al, 1999）．

3. ER-associated degradation（ERAD）

ERに蓄積したunfolded proteinを処理しきれない場合，unfolded proteinはERから細胞質にはき出され，ユビキチン化を受け，26Sプロテオソームで分解される（Bonifacino and Weissman, 1998）．

---

* 本内容は第36回日本神経精神薬理学会（2006年9月，名古屋）における，シンポジウム講演の記録である．

*1 〒565-0871 吹田市山田丘2-2 D3
E-mail: kudo@psy.med.osaka-u.ac.jp
（別刷請求先：工藤　喬）